AD-A124 716 GUST RESPONSE PREDICTION OF AN AIRFOIL USING A MODIFIED 1/1
VON(ARMAN-POHLHA..(U) AIR FORCE INST OF TECH
WRIGHT-PATTERSON AFB OH SCHOOL OF ENGI.. R G DOCKEN
UNCLASSIFIED DEC 82 AFIT/GAE/AA/82D-9 F/G 20/4 NL

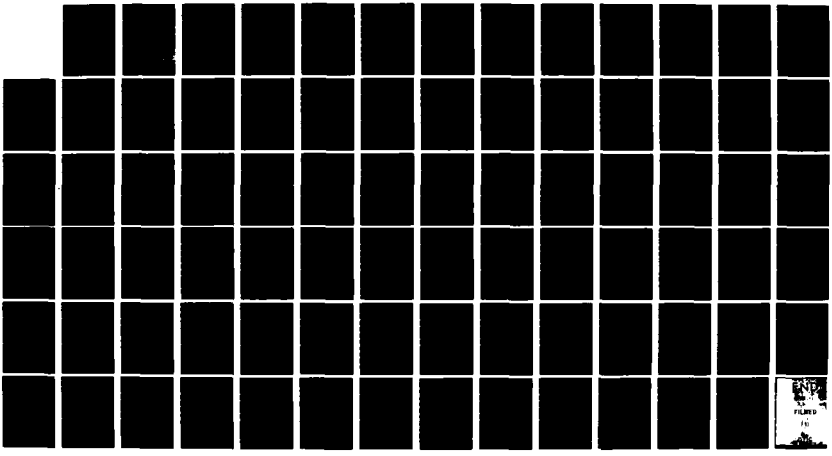

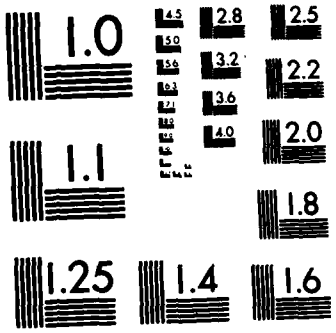

MICROCOPY RESOLUTION TEST CHART
NATIONAL BUREAU OF STANDARDS-1963-A

GUST RESPONSE PREDICTION OF AN AIRFOIL USING A MODIFIED VON KARMAN-POHLHAU EN TECHNIQUE

THESIS

Richard G. Docken, Jr.
AFIT/GAE/AA/82D-9 Capt. USAF

DEPARTMENT OF THE AIR FORCE
AIR UNIVERSITY (ATC)
AIR FORCE INSTITUTE OF TECHNOLOGY

Wright-Patterson Air Force Base, Ohio

AFIT/GAE/AA/82D-9

GUST RESPONSE PREDICTION OF AN AIRFOIL USING A MODIFIED VON KARMAN-POHLHAUSEN TECHNIQUE

THESIS

Richard G. Docken, Jr.
AFIT/GAE/AA/82D-9 Capt. USAF

Approved for public release, distribution unlimited.

AFIT/GAE/AA/82D-9

GUST RESPONSE PREDICTION
OF AN AIRFOIL
USING A MODIFIED VON KARMAN-POHLHAUSEN TECHNIQUE

THESIS

Presented to the Faculty of the School of Engineering of

the Institute of Technology

Air University

in Partial Fulfillment of the

Requirements for the Degree of

Master of Science

by

Richard G. Docken, Jr., B.S.A.A.E.

Capt. USAF

Graduate Aeronautical Engineering

December 1982

Acknowledgments

Although this thesis is the result of nine months of "Independent Study", it has by no means been an individual effort. Many people have contributed toward the success of this effort.

Many thanks go to my advisor, Major E. Jumper, whose vast knowledge in the subject area allowed for a turnaround in this effort which got us to the final conclusion presented herein. I would also like to thank Dr. J. Hitchcock, without whom the closure problem would not have been so easily solved. And I would like to thank Major M. Smith for his excellent advice and guidance on potential flow theory.

Finally, I would like to thank my wife, Debbie, for her extreme tolerance over the past nine or so months and for her tireless efforts in typing this thesis.

Richard G. Docken, Jr.

Contents

List of Symbols

C	airfoil chord
$C\ell$	lift coefficient
K	boundary layer shape parameter
m	mass flow rate
p	pressure
t	time variable
u	velocity within the boundary layer
Ue	velocity at the edge of the boundary layer
U_∞	freestream velocity
x	variable in the flow direction
y	variable normal to the flow direction
z	modified momentum thickness, $\delta_2{}^2/\nu$
α	angle of attack
$\dot{\alpha}$	angle of attack pitch rate
δ	boundary layer thickness
δ_1	displacement thickness
δ_2	momentum thickness
Λ	boundary layer shape parameter
η	non-dimensional vertical displacement, y/δ
ρ	fluid density
ν	kinematic viscosity
μ	viscosity

List of Figures

AFIT/GAE/AA/82D-9

Abstract

An analytical study is presented regarding the theoretical behavior of an airfoil in a pitching airflow. The theoretical development includes the momentum-integral equation for boundary layers in unsteady flow and the von Karman-Pohlhausen integral method for unsteady flow. A computer program was written to model this and was applied to a symmetric Joukowski airfoil. The results of this study show a linear relationship between the increase in the stall angle of attack and the non-dimensional pitch rate, $\frac{1}{2}C\dot{\alpha}/U_{\infty}$.

I Introduction

Discussion

Since the earliest days, aerodynamicists have been interested in the performance of a wing under dynamic angle of attack changes. The earliest work seems to have been most concerned with these effects as they pertained to an aircraft experiencing rapid changes in angle of attack due to the encountering of a gust (Ref. 1). More recent work seems to be concerned with these effects as they pertain to the motion of a wing in otherwise still air, and, in particular, this effect as applied to oscillatory motion as might be experienced with helicopter blades (Ref. 10).

Both of these dynamic conditions lead to an enhanced maximum lift effect; this effect, however, can be separated into two regimes. In the first, the coefficient of lift-vs-angle of attack curve ($C\ell$-vs-α) is extended up and to the right so that the maximum lift coefficient ($C\ell max$) is increased by some amount $\Delta C\ell max$. In both kinds of dynamic angle of attack change cases, the $C\ell max$ seems to be directly relatable to the non-dimensional angular rate $\frac{1}{2}C\dot{\alpha}/U_{oo}$, where C is the airfoil chord, $\dot{\alpha}$ is the pitch rate of the gust or the wing, and U_{oo} is the freestream velocity. In the second regime, a large $\Delta C\ell max$ appears as a spike superimposed on the $C\ell$-vs-α curve followed by a catastrophic decline in $C\ell$. This later effect has been attributed to the appearance of strong leading edge vortices (Ref. 10), and is beyond the scope of this effort.

This study is concerned with only the first regime. While the general trend of the effect in this regime is similar under both motions

there appears to be a measurable difference in the extent of the effect even if the restriction to constant angle of attack change rate ($\dot{\alpha}$) is fixed. In the case of a gust, constant α means that the wing is stationary, and the flow field is made to change direction at a constant rate. While in the case of the moving wing, the flow is fixed, and the wing pitches into it at a constant rate from some pivot location commonly taken as the half chord (Ref. 9).

Theoretically speaking, these two conditions differ in frame of reference, the latter being more difficult to analyze. This study is limited to the theoretical examination of the first condition; that of a fixed wing encountering a gust.

Since the phenomena of stall is due to separation of the flow from the upper surface of the wing, it is clear that a study of dynamic stall must include and, in fact, hinge upon a study of the boundary layer. The study is limited to laminar flow, but the techniques should be applicable to turbulent boundary layer flow.

Problem Statement

To set up the problem, the momentum-integral equation for boundary layer in steady flow is extended to allow for unsteady flow. Following the theoretical development, a computer program will be developed to allow one to apply this theory to certain specialized problems; namely, symmetric airfoils. The application in this study was to a Joukowski J011, an 11% thick symmetric airfoil, in order to model the flow about the leading edge of a NACA 0012 airfoil, popular in helicopter blade use. Finally, the theoretical results are compared against experimental data available in the literature (Ref. 1 and 9)

Assumptions

In order to perform the analysis, a simplifying assumption that the flow is incompressible is made. In addition, since the point of flow separation on the airfoil and the relationship to be loss of lift (aerodynamic stall) is somewhat arbitrary, in this study, aerodynamic stall is defined as when flow separation (as indicated by the shape parameter) occurs at the quarter chord point on the airfoil.

II Background

In canvassing past efforts on the dynamic stall phenomenon, it becomes apparent that the majority of the work concerns the oscillatory motion on an airfoil, which is most closely associated with helicopter blades. Other works included research on airfoils pitching into airflows. Only a few papers covered work on the gust problem, i.e. airflow pitching around an airfoil. The genisis of this work was an experiment by Max Kramer (Ref. 1).

The Kramer Experiment

In 1932, Max Kramer published a paper regarding his experiment on the dynamic stall of airfoils in pitching airflows. He got the idea after listening to several pilots commenting about the behavior of wings in unsteady airflows. To investigate these observations, he set up an experiment. In it he fixed an airfoil between a diffuser and a set of movable guide vanes (see Fig 2). The air flowed from a source, through the vanes, over the airfoil and was collected in the diffuser. The insertion of the vanes allowed Kramer to alter the direction of the airflow while taking data. This allowed him to simulate a gust encountered by an airfoil in otherwise steady flow. Kramer conducted his experiment using three different airfoils--two different profiles of the same chord and one airfoil of the same profile as one of the others but having a different chord. Kramer also ran the air at two different dynamic pressures, enabling him to obtain the pertinent characteristics involved in the problem, i.e. effect of velocity, area, camber, etc. To correlate the data, Kramer used a

non-dimensional pitch rate parameter:

$$\frac{\frac{1}{2}C\dot{\alpha}}{U_\infty}$$

where C is the chord of the airfoil, U_∞ the freestream velocity and $\dot{\alpha}$ is the pitch rate of the airflow in radians per second.

Based on his experimental results, Kramer developed an empirical relationship between the increase in $C\ell_{max}$ in the gust over $C\ell_{max}$ in steady flow and pitch rate

$$C\ell_{max_{dyn}} = C\ell_{max_{st}} + 0.36 \frac{C}{U_\infty} \frac{d\alpha}{dt}$$

(Ref. 1)

The results of Kramer's experiment have been reproduced in Figure 3.

The Deekens and Kuebler Experiment

Another experiment of interest is one conducted by two students at the Air Force Academy. In it, an airfoil (NACA 0015) was emplaced in a low speed smoke wind tunnel. Once steady flow had been established, the airfoil was pitched at a constant rate through a servo motor control (see Fig. 4). As in the Kramer experiment, a direct correlation was found between the non-dimensional pitch rate and the delay in stall angle of attack. As stated in the introduction, this is a different problem than that of the rotating airflow. The results as shown in Fig. 5 can be expressed as:

$$\Delta\alpha_{stall} = 2.1\ (\tfrac{1}{2}C\dot{\alpha}/U_\infty),$$

where C is the chord, α the angular pitch rate and U_∞ the freestream velocity. Applying classical airfoil theory, this translates to:

$$\Delta C\ell_{max} = 6.57\ C\dot{\alpha}/U_\infty, \text{ (Ref. 9:2-15)}$$

a much higher slope than that obtained by Kramer.

This is a clear indication that there are different physics governing the behavior of the airflow in each problem, and both should be pursued. This study will investigate the behavior of the airflow and boundary layer of the first case.

III Theory Development

Introduction

In deriving the theory for the gust problem, use was made of the procedures used to derive the momentum-integral equation for the boundary layer in steady flow. That derivation is reproduced in Appendix B.

The momentum-integral equation for the boundary layer is another form of the boundary layer equations that result from the simplifications of the Navier-Stokes equations that govern all flows. Thus, a procedure similar to that used to derive the boundary layer equations in general will be used here; that is, to develop the continuity equation and the momentum equation for a fluid element in the boundary layer.

The Continuity Equation

In words, the continuity principle states that the net rate of mass flow out of a control volume is equal to the time rate of loss of mass within that control volume (Ref. 2: 10). Referring to Fig. 7, this gives:

$$\int_o^h \rho u dy + \frac{\partial}{\partial x}\left(\int_o^h \rho u dy\right)dx - \int_o^h \rho u dy + \dot{m}_{o_{top}} = -\frac{\partial}{\partial t}\int_o^h \rho dy dx$$

Reducing this equation gives:

$$\dot{m}_{o_{top}} = -\frac{\partial}{\partial t}\int_o^h \rho dy dx - \frac{\partial}{\partial x}\left(\int_o^h \rho u dy\right)dx \qquad (1)$$

The Momentum Equation

The momentum principle states that the sum of the forces acting on the fluid in a control volume is equal to the net rate of transport

of momentum out of the control volume plus the time rate of change of momentum in the control volume (Ref. 2:11). Referring to Fig. 8, the x-component (parallel to the wall) of the momentum equation may be found by finding the sum of the forces in the x-direction:

$$\Sigma F = -\tau_w dx + \int_o^h p dy - \int_o^h p dy - \frac{\partial}{\partial x}\left(\int_o^h p dy\right) dx,$$

and equating it to the momentum terms

$$= \int_o^h \rho u u dy + \frac{\partial}{\partial x}\left(\int_o^h \rho u d d y\right) dx - \int_o^h \rho u u dy + \dot{m}_{o_{top}} \cdot Ue + \frac{\partial}{\partial t}\int_o^h \rho u dy dx$$

such that

$$\frac{\partial}{\partial x}\int_o^h (\rho u u) dy dx + \dot{m}_{o_{top}} \cdot Ue + \frac{\partial}{\partial t}\int_o^h \rho u dy dx = -\tau_w dx - \frac{\partial}{\partial x}\int_o^h p dy dx \quad (2)$$

Substituting for $\dot{m}_{o_{top}}$ from equation (1), equation (2) becomes:

$$\frac{\partial}{\partial x}\int_o^h (\rho u u) dy dx - Ue \cdot \frac{\partial}{\partial t}\int_o^h \rho dy dx - Ue \cdot \frac{\partial}{\partial x}\int_o^h \rho u dy dx + \frac{\partial}{\partial t}\int_o^h \rho u dy dx$$

$$= -\tau_w dx - \frac{\partial}{\partial x}\int_o^h p dy dx$$

Thus, for this two dimensional problem, the pressure gradient in the x-direction is the only pressure gradient, and correspondingly, the partial derivatives of pressure are taken as total (not substantial) derivatives. Also, since x and y are independent, the partial derivative with respect to x can be brought across the integration symbol, since the integration is in the y direction. The equation becomes

$$\int_o^h \frac{\partial}{\partial x}(\rho u u) dy dx - Ue \cdot \frac{\partial}{\partial t}\int_o^h \rho dy dx - Ue \cdot \int_o^h \frac{\partial}{\partial x}(\rho u) dy dx + \frac{\partial}{\partial t}\int_o^h \rho u dy dx$$

$$= -\tau_w dx - \int_o^h \frac{dp}{dx} dy dx \quad (3)$$

If we further restrict the flow to incompressible, the density can be divided through, as can the common dx term, so that

$$\int_o^h \frac{\partial}{\partial x}(uu)dy - Ue \cdot \frac{\partial}{\partial t}\int_o^h dy - Ue \cdot \int_o^h \frac{\partial}{\partial x} udy + \frac{\partial}{\partial t}\int_o^h udy$$

$$= -\frac{\tau_w}{\rho} - \frac{1}{\rho}\int_o^h \frac{dp}{dx}\, dy \qquad (4)$$

To this point, the only difference between this equation for unsteady flow, and the equation for steady flow is the addition of the time dependent terms. However, the next step is one of the key developments in the momentum-integral equation for the boundary layer in unsteady flow. It was at this point in the steady flow equation that Euler's equation was introduced to substitute for the pressure gradient, and the same will be done here. As shown in Appendix A:

$$-\frac{1}{\rho}\frac{dp}{dx} = Ue\frac{\partial Ue}{\partial x} + \frac{\partial Ue}{\partial t} \qquad (5) \text{ and } (A13)$$

The additional $\partial Ue/\partial t$ term introduced here is significant and will be shown to be a contributing factor in the behavior of the flow field in gusts.

It is important to note that the potential flow field in incompressible flow can and does respond instantaneously to changes, such as an angle of attack change. This is, if an airfoil is inserted in a stream at some angle of attack α_1, and the airfoil is allowed to pitch up to an angle of attack α_2, the flow field will be the same as if the airfoil was placed in a freestream at an angle of attack α_2 with no pitching. This is because, as shown in Appendix A, the velocity in potential flow is a function of α only and is not a function of time. However, the pressure gradient does not respond in this fashion. The flow field resists changes due to the inertia of the flow, in

addition to the time dependent term introduced here which causes a different kind of behavior for the pressure gradient.

Continuing on with the derivation, now substitute equation (5) into equation (4) to obtain:

$$\int_o^h \frac{\partial}{\partial x}(uu)dy - Ue \frac{\partial}{\partial t}\int_o^h dy - Ue \cdot \int_o^h \frac{\partial}{\partial x} udy + \frac{\partial}{\partial t}\int_o^h udy$$

$$= - \frac{\tau_w}{\rho} + \int_o^h Ue \frac{\partial Ue}{\partial x} dy + \int_o^h \frac{\partial Ue}{\partial t} dy$$

which, after rearranging, yields

$$- \int_o^h \frac{\partial}{\partial x}(uu)dy + Ue \frac{\partial}{\partial t}\int_o^h dy + Ue \int_o^h \frac{\partial}{\partial x} udy - \frac{\partial}{\partial t}\int_o^h udy$$

$$+ \int_o^h Ue \frac{\partial Ue}{\partial x} dy + \int_o^h \frac{\partial Ue}{\partial t} dy = \frac{\tau_w}{\rho}. \qquad (6)$$

Looking only at the time dependent terms

$$Ue \frac{\partial}{\partial t}\int_o^h dy + \int_o^h \frac{\partial Ue}{\partial t} dy - \frac{\partial}{\partial t}\int_o^h udy,$$

note that the first term, h, is an arbitrarily selected constant. When the integration is carried out and evaluated at the limits and then the partial derivative with respect to time is taken, the term is zero. In the second term, since the y-coordinate is independent of time, the partial with respect to time can be taken across the integration sign so that

$$\int_o^h \frac{\partial Ue}{\partial t} dy - \frac{\partial}{\partial t}\int_o^h udy = \frac{\partial}{\partial t}\int_o^h (Ue - u)dy. \qquad (7)$$

Now examine the spatial terms of the left hand side of equation (6):

$$- \int_o^h \frac{\partial}{\partial x}(uu)dy + Ue \int_o^h \frac{\partial u}{\partial x} dy + \int_o^h Ue \frac{\partial Ue}{\partial x} dy. \qquad (8)$$

The second term of equation (8) looks like part of

$$\int_o^h \frac{\partial(uUe)}{\partial x}\, dy$$

so that expanding this term out yields

$$\int_o^h \frac{\partial}{\partial x}(uUe)dy = \int_o^h u\,\frac{\partial Ue}{\partial x}\, dy + \int_o^h Ue\,\frac{\partial u}{\partial x}\, dy. \tag{9}$$

Note that the second term on the right hand side of equation (9) can be written

$$\int_o^h Ue\,\frac{\partial u}{\partial x}\, dy = \int_o^h \frac{\partial(uUe)}{\partial x}\, dy - \int_o^h u\,\frac{\partial Ue}{\partial x}\, dy. \tag{10}$$

Substituting (10) into (8) gives

$$-\int_o^h \frac{\partial(uu)}{\partial x}\, dy + \int_o^h \frac{\partial(uUe)}{\partial x}\, dy + \int_o^h Ue\,\frac{\partial Ue}{\partial x}\, dy - \int_o^h u\,\frac{\partial Ue}{\partial x}\, dy,$$

and combining the first two and the second two terms yields

$$\int_o^h \frac{\partial}{\partial x}(uUe - uu)dy + \int_o^h \frac{\partial Ue}{\partial x}(Ue - u)dy. \tag{11}$$

Substituting (7) and (11) into equation (6) gives

$$\int_o^h \frac{\partial}{\partial x}(uUe - uu)dy + \int_o^h \frac{\partial Ue}{\partial x}(Ue - u)dy + \frac{\partial}{\partial t}\int_o^h (Ue - u)dy = \frac{\tau_w}{\rho}.$$

The velocity gradient $\partial Ue/\partial x$ is independent of y as is the partial derivative with respect to x; thus, these can be pulled outside the integration symbol so that

$$\frac{\partial}{\partial x}\int_o^h (uUe - uu)dy + \frac{\partial Ue}{\partial x}\int_o^h (Ue - u)dy + \frac{\partial}{\partial t}\int_o^h (Ue - u)dy = \frac{\tau_w}{\rho}. \tag{12}$$

Finally, rearranging the terms, equation (12) becomes

$$\frac{\partial}{\partial x} Ue^2 \int_o^h \frac{u}{Ue}\left(1 - \frac{u}{Ue}\right) dy + Ue\,\frac{\partial Ue}{\partial x}\int_o^h \left(1 - \frac{u}{Ue}\right) dy + \frac{\partial}{\partial t} Ue \int_o^h \left(1 - \frac{u}{Ue}\right) dt = \frac{\tau_w}{\rho} \tag{13}$$

which is the momentum-integral equation for the boundary layer in unsteady flow.

IV von Karman-Pohlhausen Integration

In the preceeding chapter, the theory for the unsteady flow boundary layer was applied to develop the momentum-integral boundary layer equation for unsteady flow. The steady flow version was first integrated and applied by K. Pohlhausen in 1921. The method as used in modern texts, and that is used here, is a more modern development done in 1967 by H. Holstein and T. Bohlen (Ref. 3:206). However, the unsteady flow application has not been integrated because the addition of the transient term requires another independent equation for closure as will be evident in the analysis that follows. The closure equation can, however, be constructed, and the success with this closure equation is directly responsible for the success of this study. Since the unsteady flow method closely parallels the method for steady flow, the steady flow development of the von Karman-Pohlhausen approximate method has been reproduced in Appendix C.

The von Karman-Pohlhausen Approximate Method for Unsteady Flow

The momentum-integral equation for unsteady flow is

$$\frac{\partial}{\partial x} Ue^2 \int_o^h \frac{u}{Ue}\left(1-\frac{u}{Ue}\right)dy + Ue\frac{\partial Ue}{\partial x}\int_o^h\left(1-\frac{u}{Ue}\right)dy + \frac{\partial}{\partial t} Ue \int_o^h\left(1-\frac{u}{Ue}\right)dy = \frac{\tau_w}{\rho} \quad (13)$$

Two parameters relating to the boundary layer thickness are now introduced:

$$\delta_1 = \int_o^h\left(1-\frac{u}{Ue}\right) dy \quad (14)$$

$$\delta_2 = \int_o^h \frac{u}{Ue}\left(1-\frac{u}{Ue}\right) dy \quad (15)$$

Equation (14) represents the displacement thickness, and equation (15) represents the momentum thickness (see Fig 6). Substituting these into equation (13):

$$\frac{\partial}{\partial x} Ue^2 \delta_2 + Ue \frac{\partial Ue}{\partial x} \cdot \delta_1 + \frac{\partial}{\partial t}(Ue\ \delta_1) = \frac{\tau w}{\rho}$$

or by expanding the first term

$$2\ Ue\ \delta_2 \frac{\partial Ue}{\partial x} + Ue^2 \frac{\partial \delta_2}{\partial x} + Ue \frac{\partial Ue}{\partial x} \delta_1 + \frac{\partial (Ue\ \delta_1)}{\partial t} = \frac{\tau w}{\rho},$$

and finally rearranging yields

$$(2\delta_2 + \delta_1)\ Ue \frac{\partial Ue}{\partial x} + Ue^2 \frac{\partial \delta_2}{\partial x} + Ue \frac{\partial \delta_1}{\partial t} + \delta_1 \frac{\partial Ue}{\partial t} = \frac{\tau w}{\rho} \qquad (16)$$

As it stands, equation (16) may not be integrated in the manner of the von Karman-Pohlhausen method. In order to proceed, a closure equation must be introduced which relates the change in δ_1 with time to the change in Ue with time. To find the equation of closure, first assume that δ_1 is directly related to the boundary layer thickness:

$$\delta_1 = C_1 \delta \qquad (17)$$

which is generally true in the time domain. Then

$$\frac{\partial \delta_1}{\partial t} = C_1 \frac{\partial \delta}{\partial t}$$

As long as the flow is laminar, it can be shown that the boundary layer thickness, δ, can be related to the velocity of the potential flow, Ue, by

$$\delta = \frac{C_2 \sqrt{\nu}}{\sqrt{Ue^x}}$$

so that

$$\frac{\partial \delta_1}{\partial t} = C_1 C_2 \sqrt{\frac{\nu}{x}}\ \frac{\partial}{\partial t}\ (Ue)^{-1/2}$$

$$= C_1 C_2 \sqrt{\frac{\nu}{x}} \cdot -\frac{1}{2}\ (Ue)^{-3/2}\ \frac{\partial Ue}{\partial t}$$

$$= C_1 C_2 \sqrt{\frac{\nu}{Ue^x}} \cdot \left(- \frac{1}{2Ue} \frac{\partial Ue}{\partial t}\right)$$

$$= - \frac{\delta_1}{2Ue} \frac{\partial Ue}{\partial t} , \tag{18}$$

as long as the time dependence of C_1 and C_2 are small as compared to that of Ue, which is somewhat restrictive. Equation (18) thus forms the closure equation necessary to put the unsteady integral equation in manageable form. Substituting equation (18) into equation (16) yields

$$(2\delta_2 + \delta_1)\, Ue \frac{\partial Ue}{\partial x} + Ue^2 \frac{\partial \delta_2}{\partial x} + \delta_1 \frac{\partial Ue}{\partial t} - \frac{1}{2} \delta_1 \frac{\partial Ue}{\partial t} = \frac{\tau_w}{\rho} . \tag{19}$$

Equation (19) is then multiplied through by δ_2/ν:

$$\left(2 + \frac{\delta_1}{\delta_2}\right) \frac{\delta_2^2}{\nu} Ue \frac{\partial Ue}{\partial x} + Ue^2 \frac{\delta_2}{\nu} \frac{\partial \delta_2}{\delta x} + \frac{1}{2}\left(\frac{\delta_1}{\delta_2}\right) \frac{\delta_2^2}{\nu} \frac{\partial Ue}{\partial t} = \frac{\tau_w \delta_2}{\mu} ,$$

and divided through by Ue:

$$\left(2 + \frac{\delta_1}{\delta_2}\right) \frac{\delta_2^2}{\nu} \frac{\partial Ue}{\partial x} + Ue \frac{\delta_2}{\nu} \frac{\partial \delta_2}{\partial x} + \frac{1}{2Ue}\left(\frac{\delta_1}{\delta_2}\right) \frac{\delta_2^2}{\nu} \frac{\partial Ue}{\partial t} = \frac{\tau_w \delta_2}{\mu Ue} . \tag{20}$$

Finally:

$$\left(2 + \frac{1}{2} \frac{\delta_1}{\delta_2}\right) \frac{\delta_2^2}{\nu} \frac{1}{Ue} \frac{\partial Ue}{\partial t}$$

is added and subtracted to get

$$\left(2 + \frac{\delta_1}{\delta_2}\right) \frac{\delta_2^2}{\nu} \left(\frac{\partial Ue}{\partial x} + \frac{1}{Ue} \frac{\partial Ue}{\partial t}\right) + \frac{Ue \delta_2 \delta_2'}{\nu} - \left(2 + \frac{1}{2} \frac{\delta_1}{\delta_2}\right) \frac{\delta_2^2}{\nu} \frac{1}{Ue} \frac{\partial Ue}{\partial t} = \frac{\tau_w \delta_2}{\mu Ue} \tag{21}$$

To make a boundary layer computation, some information must first be determined concerning δ_1 and δ_2; however, these parameters are in terms of an as yet undetermined velocity profile within the boundary layer. The velocity profile must satisfy two constraints:

a. The order of the velocity equation must be of an order compatible with the number of boundary conditions.

b. The velocity profile must allow for an inflexion point since the flow will be with a pressure gradient (Ref. 8).

$$y = 0 \qquad u = 0 \tag{22a}$$

$$\nu\partial^2 u/\partial y^2 = -\,Ue\ \partial Ue/\partial x + \partial Ue/\partial t \tag{22b}$$

$$y = \delta \qquad u = Ue \tag{22c}$$

$$\partial u/\partial y = 0 \tag{22d}$$

$$\partial^2 u/\partial y^2 = 0 \tag{22e}$$

Note that except for the second boundary condition, these are all identical to the steady flow boundary conditions. The second boundary condition is altered only to account for the unsteady pressure term from Euler's equation as developed in the Appendix.

The existence of five boundary conditions allows for a fourth degree polynomial expression for the velocity profile:

$$\frac{u}{Ue} = A + B\eta + C\eta^2 + D\eta^3 + E\eta^4, \tag{23}$$

where $\eta = y/\delta$.

Applying (22a) gives

$$A = 0, \tag{24a}$$

and (22c) yields

$$1 = B + C + D + E. \tag{24b}$$

Now, applying (22d)

$$0 = B + 2C + 3D + 4E \tag{24c}$$

and applying (22e)

$$0 = 2C + 6D + 12E. \tag{24d}$$

Finally, equation (22b) is applied to get

$$\frac{Ue}{\delta}\frac{\partial(u/Ue)}{\partial(y/\delta)} = B + 2C\eta + 3D\eta^2 + 4E\eta^3$$

$$\frac{Ue}{\delta^2}\frac{\partial^2(u/Ue)}{\partial(y/\delta)^2} = 2C + 6D\eta + 12E\eta^2\Big|_{\eta=0}$$

$$2C = \frac{-\delta^2}{\nu}\left(\frac{\partial Ue}{\partial x} + \frac{1}{Ue}\frac{\partial Ue}{\partial t}\right) \tag{24e}$$

At this point, a dimension less parameter, Λ, is introduced and defined as:

$$\Lambda = \frac{\delta^2}{\nu}\left(\frac{\partial Ue}{\partial x} + \frac{1}{Ue}\frac{\partial Ue}{\partial t}\right) \tag{25}$$

Notice that Λ here is different from that defined for steady flow. Substituting (25) into equation (24d) and solving the equations (24a-d) yields

$$A = 0$$

$$B = 2 + \Lambda/6$$

$$C = \quad - \Lambda/2$$

$$D = -2 + \Lambda/2$$

$$E = 1 - \Lambda/6$$

These are exactly the results obtained for the steady flow boundary layer velocity profile. This should not be surprising in that one should expect to recover the steady flow solution from the unsteady flow solution if, in fact, the unsteady flow terms are dropped. This is what happens if the unsteady term is dropped from the definition of Λ.

The details of how to solve for the constants are in Appendix D.

The velocity profile becomes:

$$\frac{u}{Ue} = \left(2\eta - 2\eta^3 + \eta^4\right) + \Lambda/6\left(\eta - 3\eta^2 + 3\eta^3 - \eta^4\right)$$

and δ_1 and δ_2 can now be solved:

$$\frac{\delta_1}{\delta} = \frac{1}{\delta}\int_0^h \left(1 - \frac{u}{Ue}\right) dy.$$

For $y>\delta$, $u=Ue$ by the definition of boundary layer, and integration beyond that point gains no additional information. Thus, the integration

to $h>\delta$ gives a result identical to an integration only to $h=\delta$. Thus,

$$\frac{\delta_1}{\delta} = \int_0^1 \left(1 - \frac{u}{Ue}\right) dy,$$

Substituting η into the momentum thickness and adjusting the integration limits accordingly yields

$$\frac{\delta_1}{\delta} = \int_0^1 \left(1 - \frac{u}{Ue}\right) d\eta,$$

and substituting for u/Ue gives

$$\frac{\delta_1}{\delta} = \int_0^1 \left[1-(2\eta - 2\eta^3 + \eta^4) - \frac{\Lambda}{6}(\eta - 3\eta^2 + 3\eta^3 - \eta^4)\right] d\eta;$$

$$\frac{\delta_1}{\delta} = \frac{3}{10} - \frac{\Lambda}{120} \tag{26}$$

and similarly,

$$\frac{\delta_2}{\delta} = \int_0^1 \left[(2 - 2\eta^3 + \eta^4) + \frac{\Lambda}{6}(\eta - 3\eta^2 + 3\eta^3 - \eta^4)\right] \cdot \left[1-(2\eta - 2\eta^3 + \eta^4) - \frac{\Lambda}{6}(\eta - 3\eta^2 + 3\eta^3 - \eta^4)\right] d\eta$$

$$\frac{\delta_2}{\delta} = \frac{37}{315} - \frac{\Lambda}{945} - \frac{\Lambda^2}{9072} \tag{27}$$

The details of the integration are presented in Appendix D. The shear stress at the wall is defined as:

$$\tau_w = \frac{\mu \partial u}{\partial y}\bigg|_{y=0};$$

or

$$\frac{\tau_w \delta}{\mu Ue} = \frac{\partial (u/Ue)}{\partial (y/\delta)}\bigg|_{\eta=0} = 2 + \frac{\Lambda}{6} \tag{28}$$

The separation criteria can now be determined, as separation is defined as the point where the shear stress as measured at the wall is zero so that

$$2 + \Lambda/6 = 0$$

i.e.,

$$\Lambda = -12 \tag{29}$$

The momentum-integral equation in its last form was:

$$\left(2+\frac{\delta 1}{\delta 2}\right)\frac{\delta 2^2}{\nu}\left(\frac{\partial Ue}{\partial x}+\frac{1}{Ue}\frac{\partial Ue}{\partial t}\right)+\frac{Ue\delta 2\delta 2'}{\nu}-\left(2+\frac{1}{2}\frac{\delta 1}{\delta 2}\right)\frac{\delta 2^2}{\nu}\frac{1}{Ue}\frac{\partial Ue}{\partial t}=\frac{\tau w\delta 2}{\mu Ue} \quad (21)$$

By introducing another dimensionless parameter, K, defined by

$$K \equiv z\left(\frac{\partial Ue}{\partial x}+\frac{1}{Ue}\frac{\partial Ue}{\partial t}\right) \quad (30a)$$

or

$$K \equiv \frac{\delta 2^2}{\nu}\left(\frac{\partial Ue}{\partial x}+\frac{1}{Ue}\frac{\partial Ue}{\partial t}\right) \quad (30b)$$

the right hand side of equation (21) becomes

$$\frac{\tau w\delta 2}{\mu Ue}=\frac{\tau w\delta}{\mu Ue}\cdot\frac{\delta 2}{\delta}$$

$$=\left(2+\frac{\Lambda}{6}\right)\left(\frac{37}{315}-\frac{\Lambda}{945}-\frac{\Lambda^2}{9072}\right)\equiv f_2(K) \quad (31)$$

and similarly,

$$K=\frac{\delta^2}{\nu}\left(\frac{\partial Ue}{\partial x}+\frac{1}{Ue}\frac{\partial Ue}{\partial t}\right)\left(\frac{\delta 2}{\delta}\right)^2 ;$$

$$K=\left(\frac{37}{315}-\frac{\Lambda}{945}-\frac{\Lambda^2}{9072}\right)^2\Lambda \quad (32)$$

Finally,

$$\frac{\delta 1}{\delta 2}=\frac{\delta 1}{\delta}\cdot\frac{\delta}{\delta 2}=\left(\frac{2}{10}-\frac{\Lambda}{120}\right)\left(\frac{37}{315}-\frac{\Lambda}{945}-\frac{\Lambda^2}{9072}\right)^{-1} \quad (33a)$$

$$\frac{\delta 1}{\delta 2}\sim f_1(K) \quad (33b)$$

Substituting into equation (21) yields

$$\left[2+f_1(K)\right]K+\frac{Ue\delta 2\delta 2'}{\nu}-\left[2+\frac{1}{2}f_1(K)\right]\frac{Z}{Ue}\frac{\partial Ue}{\partial t}=f_2(K) \quad (34)$$

Now,

$$\frac{Ue\delta 2\delta 2'}{\nu}=\frac{1}{2}\frac{Ue}{\nu}\frac{d(\delta 2^2)}{dx}$$

or

$$\frac{Ue\delta 2\delta 2'}{\nu}=\frac{1}{2}Ue\left(dz/dx\right) \quad (35)$$

Substituting (35) into (34) gives

$$\left[2+f_1(K)\right]\cdot K + \frac{Ue}{2}\frac{dz}{dx} - \left[2+\frac{1}{2}f_1(K)\right]\frac{Z}{Ue}\frac{\partial Ue}{\partial t} = f_2(K)$$

$$Ue\frac{dz}{dx} - \left[4+f_1(K)\right]\frac{Z}{Ue}\frac{\partial Ue}{\partial t} = 2f_2K - 4K - 2f_1(K)\cdot K \qquad (36)$$

The right hand side of equation (36) can be defined as:

$$2f_2K - 4K - 2Kf_1(K) \equiv F(K) \qquad (37)$$

which again is identical in form to the steady flow solution. Indeed the steady flow solution can be recovered if the unsteady terms are dropped. So that substitution of equation (37) into equation (36) finally gives

$$\frac{dz}{dx} = \left[F(K) + \left[4+f_1(K)\right]\frac{Z}{Ue}\frac{\partial Ue}{\partial t}\right]\frac{1}{Ue} \qquad (38a)$$

$$Z = K\left(\frac{\partial Ue}{\partial x} + \frac{1}{Ue}\frac{\partial Ue}{\partial t}\right)^{-1} \qquad (38b)$$

which are the modified equations to be used to solve the boundary layer using the method of von Karman-Pohlhausen. Again, it is interesting to note how the steady flow solution is recovered if only the unsteady terms are dropped from the equations.

As in the steady flow solution method, the integration procedure begins at the stagnation point, where Ue=0. In this study, the stagnation point conditions are computed in the absence of unsteady flow so that as in the steady flow case F(K) must be zero so that dz/dx at the stagnation point is finite. Solving (67) for F(K)=0, and for steady flow gives

$$\Lambda_o = 7.052 \qquad (39a)$$

$$K_o = 0.077 \qquad (39b)$$

Then, $Z_o = \frac{0.077}{Ue^1}$, and $\left.\frac{dz}{dx}\right|_o = \frac{0}{0}$. Using the limit (Ref. 3:211):

$$\frac{dz}{dx} = -\ 0.0652\ U_o''/(U_o')^2$$

Now, to complete the discussion on the Pohlhausen integration, the steps to integrate the boundary layer are:

1. Compute the velocity, Ue, velocity gradient, $\partial Ue/\partial x$ and $\partial Ue/\partial t$ using the potential flow solution about an airfoil. See Appendix A for details.

2. Knowing z_o and dz/dx, find z_1:

$$z_1 = z_o + \left.\frac{dz}{dx}\right|_o \cdot dx,$$

where dx is an increment of arc length along the airfoil.

3. Compute a new value of K from equation (38b). At this point, the value of Λ can be backed out from equation to determine flow attachment or separation (32). However, since Λ for separation is known, as is $K = K(\Lambda)$, then K for separation can be determined and thus allow the elimination of one step in the integration process. This is done for this study; $K_{sep} = -\ 0.1567$ (Ref. 3:212).

4. F(K) is determined by:

   a) Knowing Λ and solving equation (32), (33), (34) and finally (37), or,

   b) Approximating F(K) vs K by a linear approximation:

      $F(K) = a - bK$

      where $a = .47$

      $b = 6$ (Ref. 3:213)

      Method (b) was chosen for this study.

5. Knowing F(K) from the linear approximation and Ue and $\partial Ue/\partial t$ from the potential flow solution, f(K) by equation (33), and the current value of z, a new dz/dx is computed.

6. Knowing z_i and having computed $dz/dx\big|_i$; z_{i+1} is computed by

$$z_{i+1} = z_i + dz/dx\big|_i \cdot dx$$

7. Repeat steps 3 - 6 with steady flow only until the boundary layer develops numerically approximately a 1-degree arc along the airfoil. Then, repeat steps 3 - 6 using the unsteady methods until the 1/4-chord is reached. Check K for separation. If the flow is attached, increment the angle of attack and repeat until separation occurs. Then choose a different pitch rate and repeat again until separation occurs. As separation is reached each time, record velocity, pitch parameter, and angle of attack at flow separation.

Results

Discussion

No theoretical investigation would be complete without a demonstration of how well that theory performed against measured results. As discussed in Chapter II, there are two experiments on record that concern a pitching airfoil and pitching airflow, and each one shows a positive correlation between this pitching and either the delay in stall angle of attack or the enhancement of maximum lift coefficient.

To demonstrate the validity of the theory developed in this study, the modified von Karman-Pohlhausen integral method was programmed on the AFIT/Harris 500 computer (see Appendix E). In the unsteady flow Pohlhausen method, the velocity Ue, the time dependent velocity variation $\partial Ue/\partial t$, and velocity gradient, $\partial Ue/\partial x$ are required. However, to determine these, a specific geometry must be defined. To do this, an 11% thick symmetric Joukowski airfoil (J011) was chosen as a model for application. A Joukowski airfoil was chosen because it has its origins in complex potential flow theory, and the necessary information (i.e. Ue, $\partial Ue/\partial x$, and $\partial Ue/\partial t$) is easily computed without requiring some of the other laborious techniques required to model the flow over (real) airfoils. Besides, one of the goals is to apply the theory to a representative problem (and not necessarily an exact problem) to determine how the theory works. For the section of the airfoil being used in the analysis, it is for all intents and purposes an exact problem without having to be concerned with the trailing edge cusp.

To approximate the required derivatives, several methods can be used; namely, forward difference, backward difference, and central

difference. It has been noted that the variation in accuracy of either of these differences when applied in the Pohlhausen integration, is insignificant (Ref. 4). Thus, a central difference was chosen for $\partial U/\partial x$:

$$\frac{\partial U}{\partial x} = \frac{U_{i+1} - U_{i-1}}{d\delta_{i+1} - d\delta_{i-1}} ,$$

and a backward difference scheme was chosen for the time variation

$$\frac{\partial U}{\partial t} = \frac{U_i - U_{i-1}}{\Delta t} , \text{ where } \Delta t = \frac{d\delta_{i-1}}{U_i - 1}$$

Results

The program was run at three different velocities, and at each velocity, four different pitch rates were chosen. These were input semi-interactively into the program. The output consisted of several columns of data, such as velocity, velocity gradient, etc. Of special importance was the column of values of K. The computation ceased at the quarter chord, at which point K was checked. If K was within a few precent of the stall indication (K = - .1567), the angle and pitch parameter were recorded and plotted (see Fig. 9). The 16 runs that resulted in separation at the quarter chord are plotted in Fig. 9. The figure points out a few very important details:

1. The relationship between the delayed stall angle and pitch rate is linear, as shown experimentally.
2. There is no change in the effect with respect to velocity of the freestream, when the pitch rate is non-dimensionalized.

These results, while seemingly subtle, are indeed profound in that they allow us to say that a theoretical tool for prediction of

this phenomena; namely, gust response of an airfoil, does exist.

Another result, shown in Fig. 10, is the contribution the transient term $\partial Ue/\partial t$ in the Euler equation of motion makes to the behavior of the flow. In Fig. 10, the shape factor for both steady and unsteady flow are plotted against chord location for a typical run. Now, in steady flow, only $\partial Ue/\partial x$ contributes to the shape factor, K; whereas, in unsteady flow, both $\partial Ue/\partial x$ and $\left({}^{1}/Ue\right) \cdot \partial Ue/\partial t$ contribute. Since at stagnation, K = 0.0770, and at separation K = - 0.1567, it is obvious that a less negative value of K results in better behaved (attached) boundary layer flow. As seen in Fig. 10, this is exactly the effect of ${}^{1}/Ue \cdot \partial Ue/\partial t$--to make the shape factor less negative. Thus, a third observation can be made:

3. The transient term $\left({}^{1}/Ue\right) \cdot \partial Ue/\partial t$, in the unsteady Euler equation of motion, has a positive effect in maintaining an attached boundary layer resulting in a delay in the stall angle of attack.

Comparison with Experiment

As discussed in Chapter II, Kramer formulated a relationship to relate gust pitch rate to the delay in stall angle. This was given as:

$$C\ell_{max_{dyn}} = C\ell_{max_{st}} + 0.36 \frac{C}{U_\infty} \dot{\alpha}$$

where $\dot{\alpha}$ is in radians/second. Referring to Fig. 9, the results of the theoretical study show that

$$\alpha stall_{dyn} = \alpha stall_{st} + 16.00 \cdot \frac{\frac{1}{2}C\dot{\alpha}}{U_\infty} .$$

If this is converted to radians:

$$\alpha_{s_{dyn}} = \alpha_{s_{st}} + 0.28 \frac{\frac{1}{2}C}{U_\infty} \dot{\alpha}.$$

To compare this to the Kramer experiment, the relationship must reflect not the difference in stall angle of attack, but rather the maximum lift coefficient. To get the results obtained in this study into the form that Kramer had, let it be assumed that the slope $C\ell_\alpha$ in the linear region of the $C\ell$-vs-α curve be continued upward and to the right at the same slope so as to relate $\Delta\alpha_{stall}$ and $\Delta C\ell_{max}$. If this is assumed, and classic airfoil theory is applied (i.e. $C\ell_\alpha$ = 2π/radian), then the results of this study can be expressed as:

$$\Delta C\ell_{max} = 0.878 \frac{C\dot{\alpha}}{U_\infty} ,$$

where the factor of ½ has been included in the slope as was done in Kramer's experiment (Ref. 1).

The slope is considerably greater as determined by the theory. However, it must be noted that Kramer did his experiments on actual wing surfaces and not true airfoils. These wings had aspect ratios on the order of 1.5. Thus, if three dimensional flow corrections (Ref. 11:2-6 and 2-7) are made to the results of this study, a comparitive result is:

$$\Delta C\ell_{max} = 0.343 \frac{C\dot{\alpha}}{U_\infty} .$$

This gives a remarkably close result when compared to Kramer's experiment. However, the actual aspect ratio of Kramer's test wings was eyeballed, and the actual values are not specified in his report. Thus, the corrected slope for the results of this study could fall within a range of 0.263 to 0.405, depending on the value of the aspect ratio chosen.

VI Conclusions and Recommendations

Conclusions

1. There exists a positive correlation between gust pitch rate and the delay in the stall angle of attack--the so-called dynamic stall angle of attack.

2. Existing steady flow theory can be successfully modified to mathematically explain this phenomena. In conjunction with this, existing integral methods can also be modified to model this phenomena.

3. For the von Karman-Pohlhausen integral method used in this study, the equation of closure exists to successfully complete the transient flow modification, without introducing significant approximations as to the relative dominance of some terms vs others.

4. With only a slight variation in slope of the respective curves there now exists both an experimental demonstration and a numerically proven analytical explanation of the physics of gust flow response of an airfoil that heretofore did not exist.

5. Since the potential flow acts in a linear fashion, the pitching airflow really does not change the dynamics. Therefore, it must be the pressure gradient in unsteady flow as determined from Euler's equation that controls the behavior of the stall dynamics in this environment.

Recommendations

As in any study, the end of this effort does not also mean the end of the investigation. The end of this study should be the foundation for many future efforts. Some of those efforts particularly highlighted by this study are:

1. In developing the equation of closure, it was assued that the time dependence of the constants C_1 and C_2 was small compared to the time dependence of Ue. This approximation needs to be studied further and reported on.

2. In the execution of the von Karman-Pohlhausen method for unsteady flow, it was assumed that the behavior of δ_1/δ_2 was not affected by the time dependent nature of the flow. This may or may not be true, and must be examined further.

3. It would be interesting to execute the same problem using a modern computational numerical method and to compare the complexity of development of each, compare the efficiency of the computer program for the numerical method to the computer program developed for this study, and to comment on regimes of applicability.

4. The Deekens and Kuebler experimental investigation, the pitching airfoil, has yet to be mathematically modelled. The two major problem areas that need to be investigated before the total physics can be understood are:

a) derivation of a suitable governing equation that adequately describes the boundary layer when the airfoil is pitched; and

b) the determination of the appropriate boundary condition or conditions as applied to this governing equation.

5. In trying to relate the results of this study to those of Kramer, it was assumed that the slope of $C\ell$ vs. α between $C\ell_{max_{dyn}}$ and $C\ell_{max_{st}}$ is the same as it is for $C\ell_{\alpha}$ in the steady flow regime. This may or may not be true, and this relationship must be studied, either analytically or experimentally, and reported on.

6. In modeling the airflow, the trailing edge (starting) vortex that is shed when the airflow pattern changes about the airfoil (as is the case in this study) was not included. These starting vortices are necessary to satisfy Helmholtz' Vortex Theorems and are physically observed (Ref. 12:53-55). In this study, the effect of these was assumed to be small, but this assumption may need further study (Ref. 13:379-390 and Ref. 14:376-378).

Bibliography

1. Kramer, Von Max "The Increase of $C\ell_{max}$ of Airfoils with a Sudden Increase in Angle of Attack Gust Effect", English translation, 14 April, 1932.

2. Hankey, W.L. "Introduction to Computational Aerodynamics", Air Force Institute of Technology, July 1981.

3. Schlicting, H. Boundary Layer Theory, Seventh Edition, McGraw-Hill Book Company, 1979.

4. Ruth, F.D. Class Notes for AE7.26, "Boundary Layer Theory", School of Engineering, Air Force Institute of Technology, 1973.

5. Smith, M. Class Notes for AE6.36, "Airfoil and Wing Theory", School of Engineering, Air Force Institute of Technology, 1982.

6. Schlicting, J., and Truckenbrodt, E. Aerodynamics of the Airplane, McGraw-Hill International Book Company, 1979.

7. Karamcheti, K. Principles of Ideal Aerodynamics, Robert E. Krieger Publishing Company, 1980 Edition.

8. Hankey, W.L. Class Notes for AE7.51, "Computational Fluid Dynamics", School of Engineering, Air Force Institute of Technology, 1982.

9. Deekens, A.C., and Kuebler, W.R. "A Smoke Tunnel Investigation of Dynamic Separation", Air Force Academy Aeronautics Digest - Fall 1978, February 1979.

10. Koltapalli, S.B.R., and Pierce, G.A. "Drag on an Oscillating Airfoil in a Fluctuating Freestream", Nonsteady Fluid Dynamics, Dec. 1978.

11. Nicolai, L. Fundamentals of Aircraft Design, distributed by METS, Inc., 1975.

12. Kuethe, A.C., and Chow, C. Foundations of Aerodynamics: Basis of Aerodynamic Design, Third Edition, John Wiley & Sons, 1976.

13. von Karman, T., and Sears, W.R. "Airfoil Theory for Non-Uniform Motion", Journal of Aeronautical Sciences, Volume 5, Number 10, August 1938.

14. Kuethe, A.C., and Sears, W.R. "The Growth of Circulation of an Airfoil Flying Through a Gust", Journal of Aeronautical Sciences, Volume 6, Number 9, July 1939.

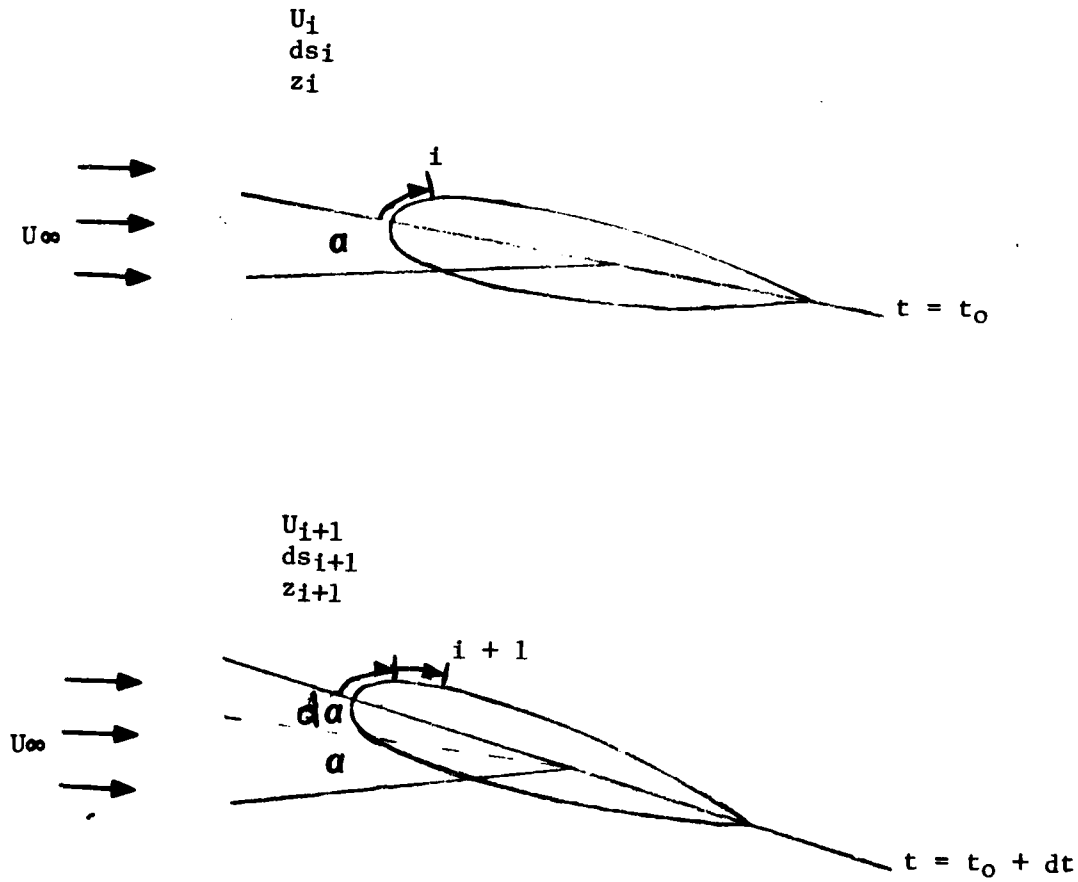

Figure 1. Transient Analysis Procedure

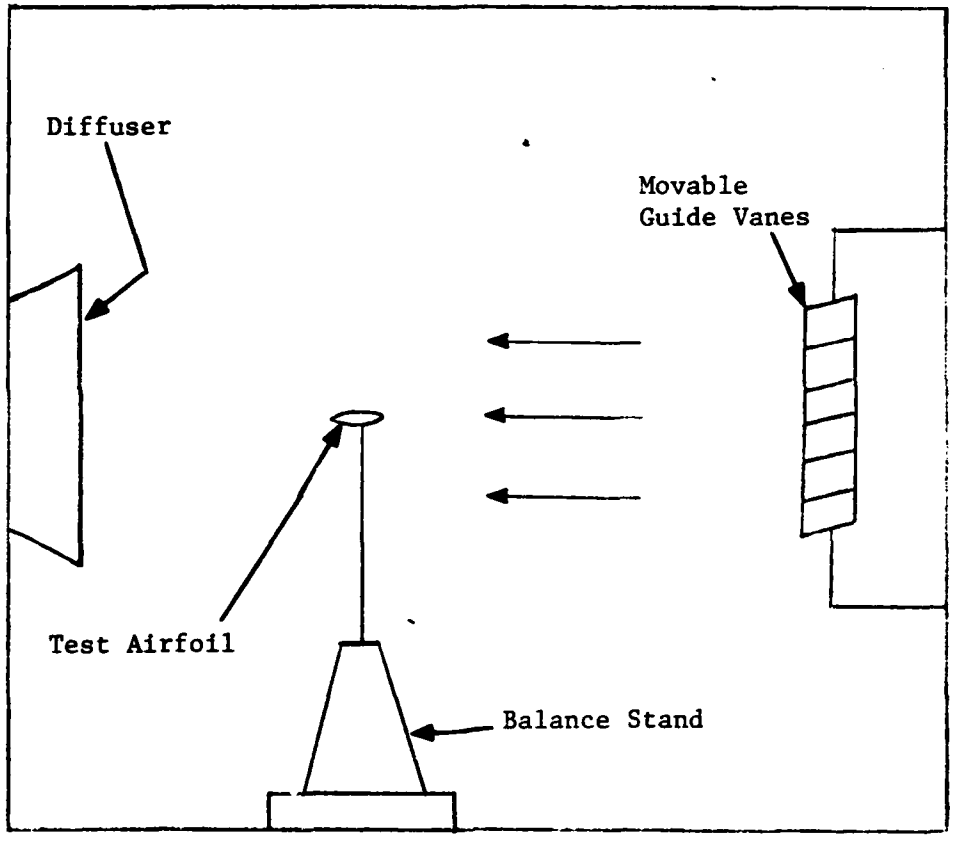

Figure 2. Schematic of Kramer Experiment

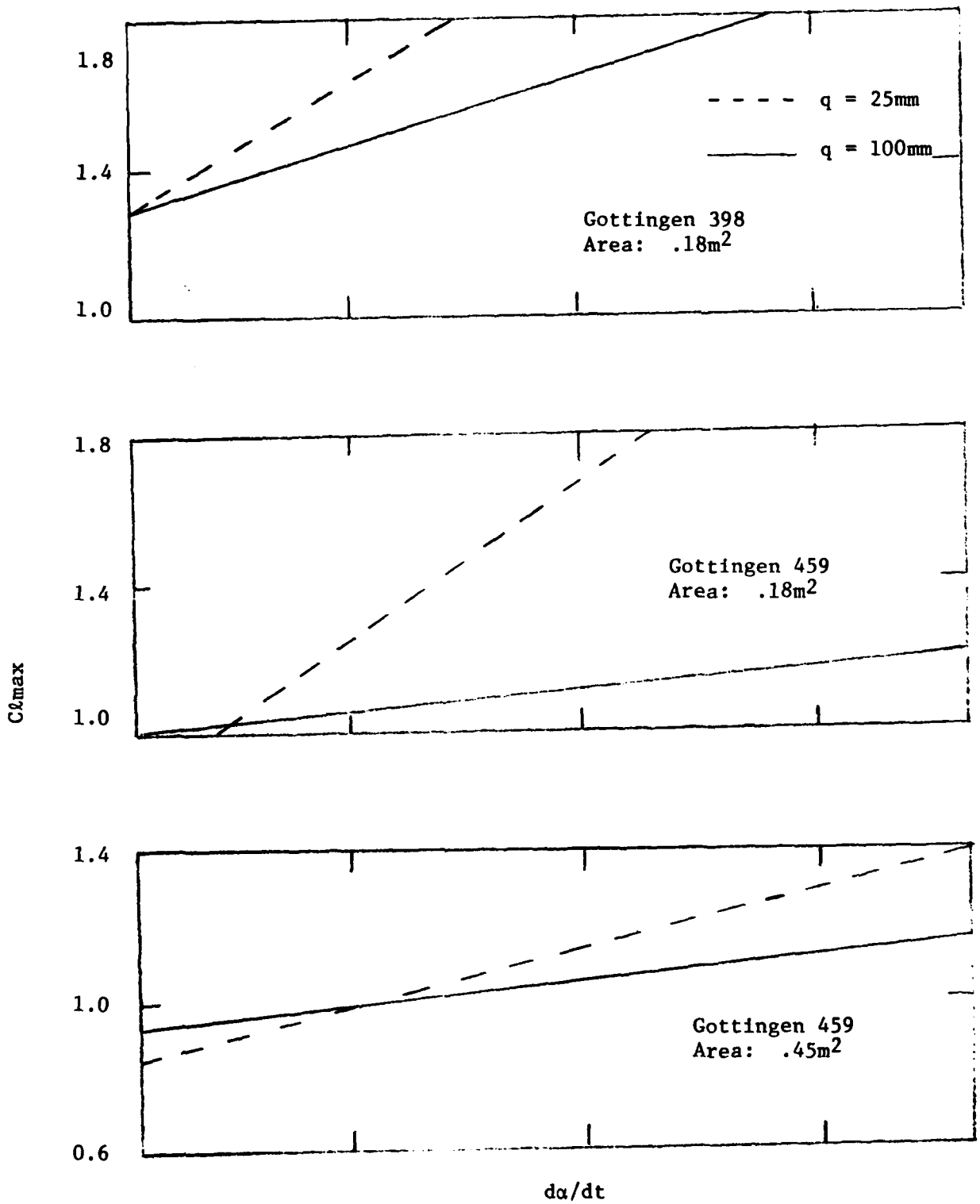

Figure 3. Summary of Kramer's Results - Effect of Pitch Rate on $C\ell max_{dyn}$

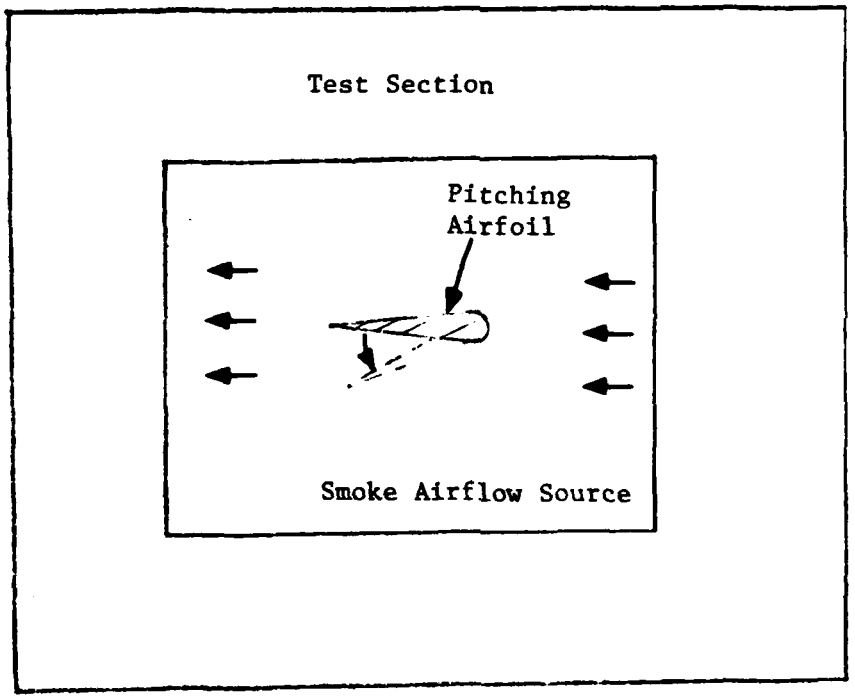

Figure 4. Schemtic of the Deekens and Kuebler Experiment

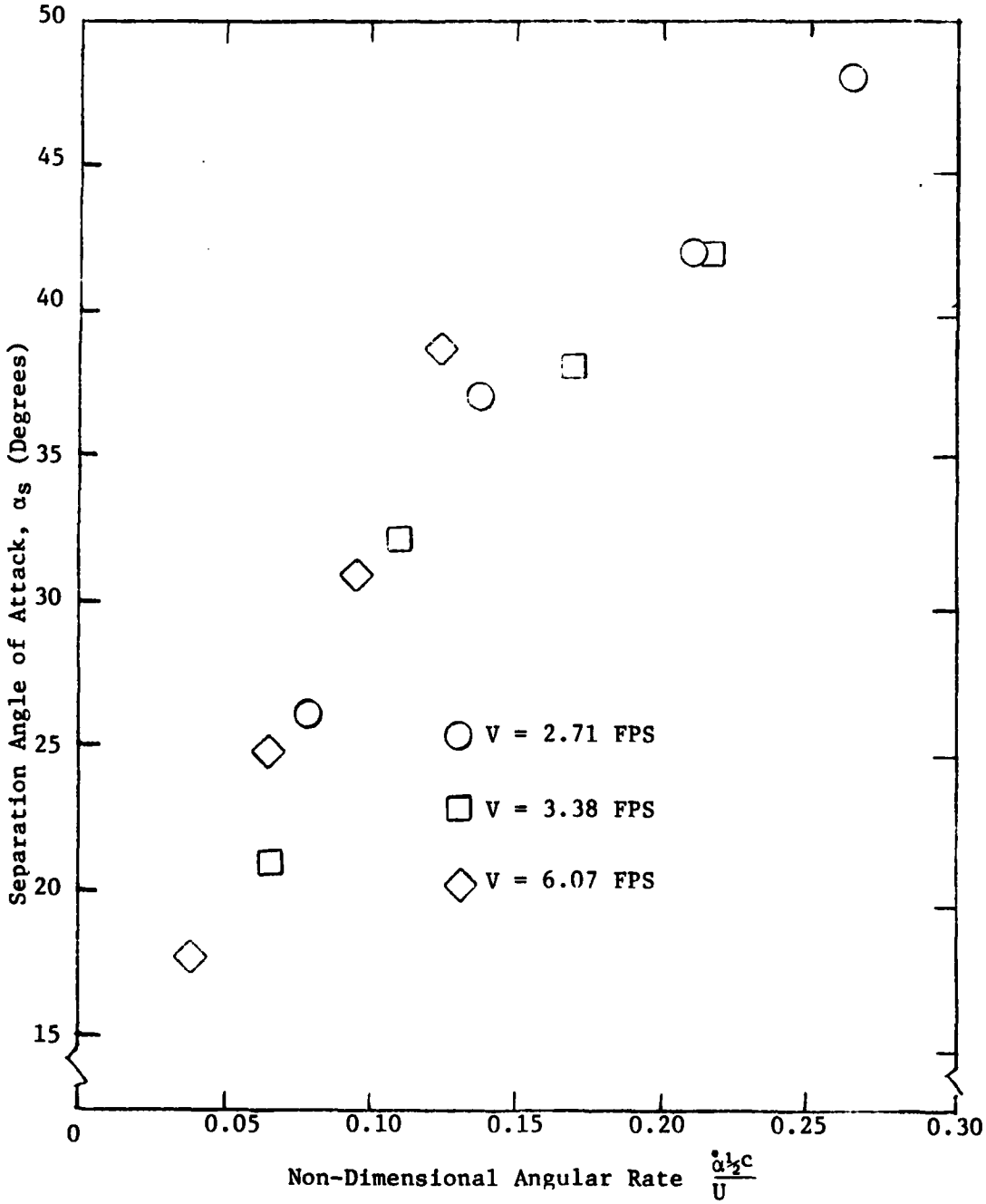

Figure 5. Results of the Deekens and Kuebler Experiment - Effect of Pitch Rate on $\Delta\alpha_{stall}$

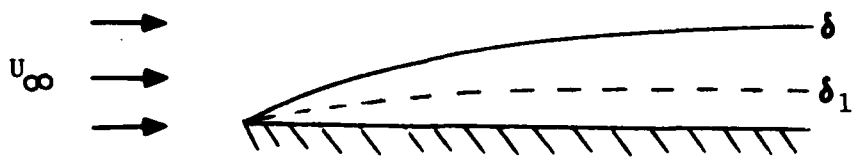

a. Displacement Thickness Compared to Boundary Layer Thickness

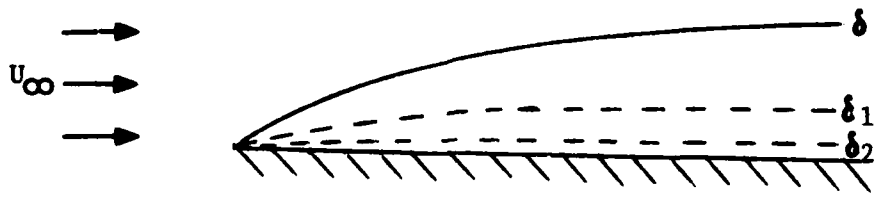

b. Momentum Thickness Compared to Displacement Thickness and Boundary Layer Thickness

Figure 6. Relative Comparison of the Boundary Layer Thickness, Displacement Thickness, and Momentum Thickness

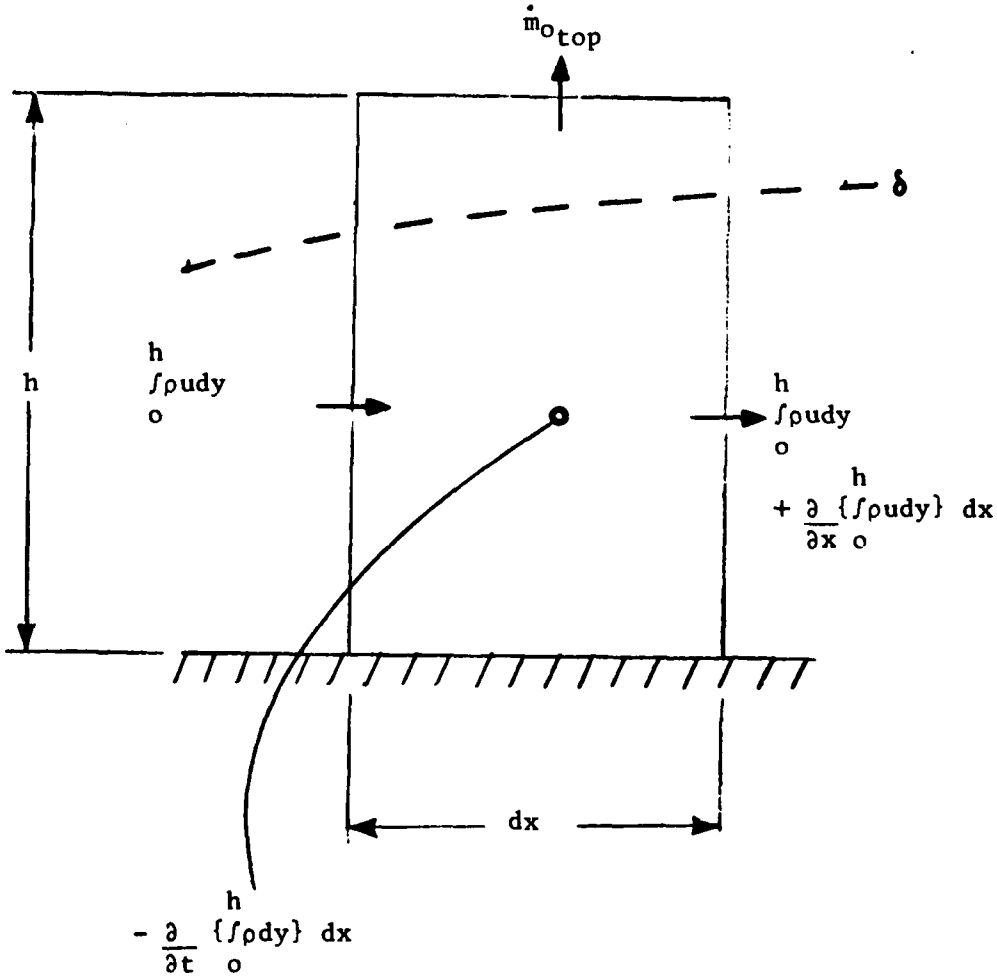

Figure 7. Fluid Volume Element
Used for the Continuity Equation

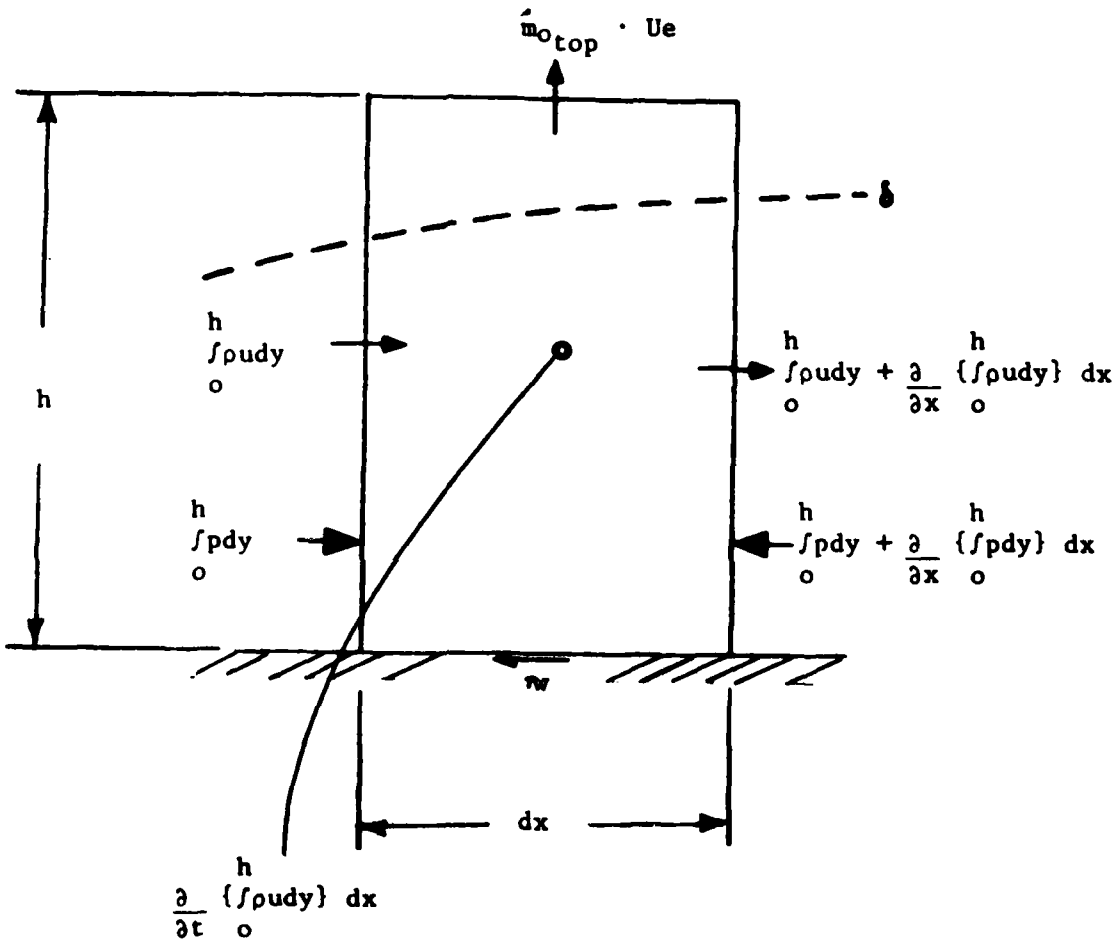

Figure 8. Fluid Volume Element
Used for the Momentum Equation

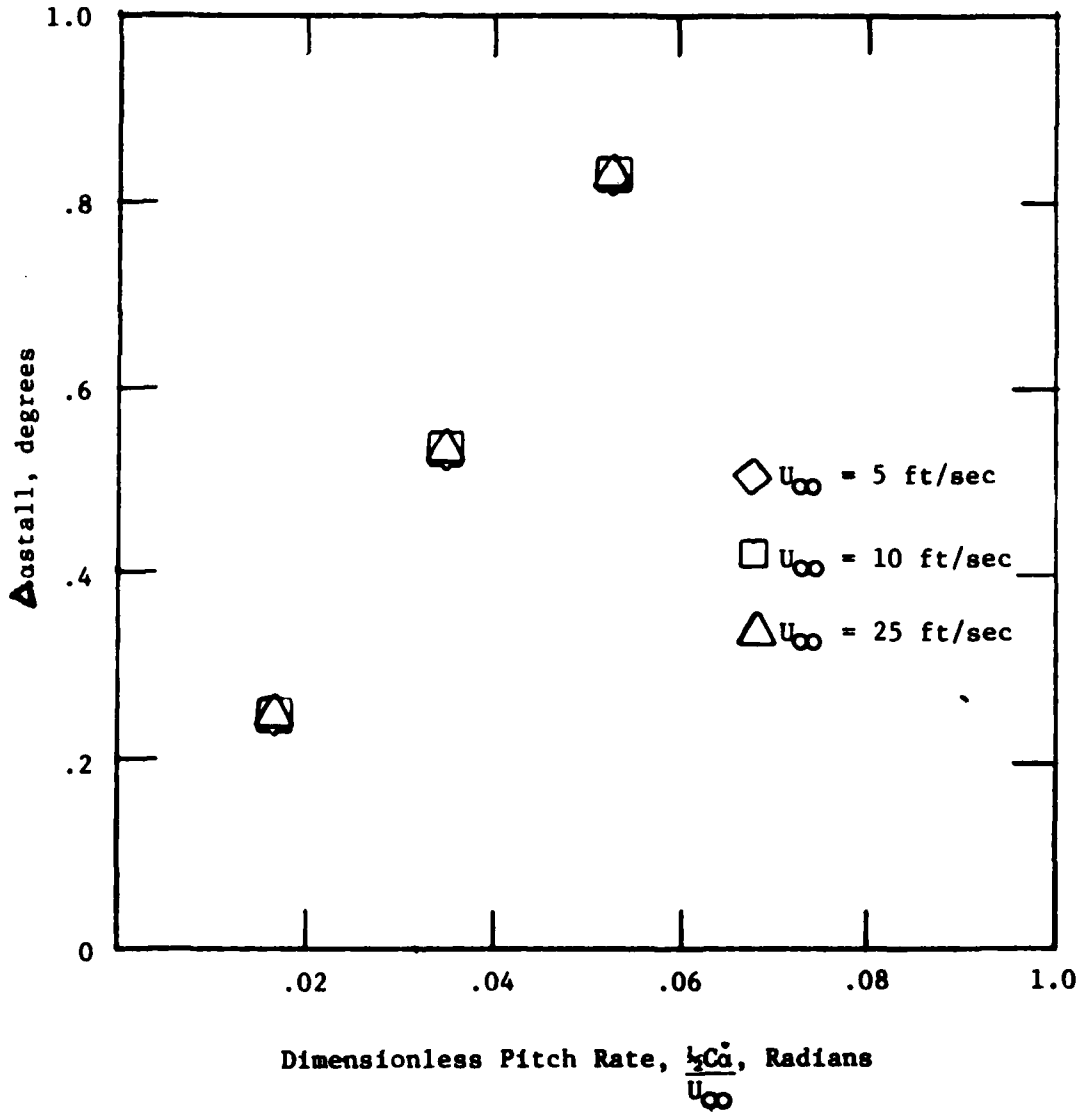

Figure 9. Effect of Pitching Airflow on αstall

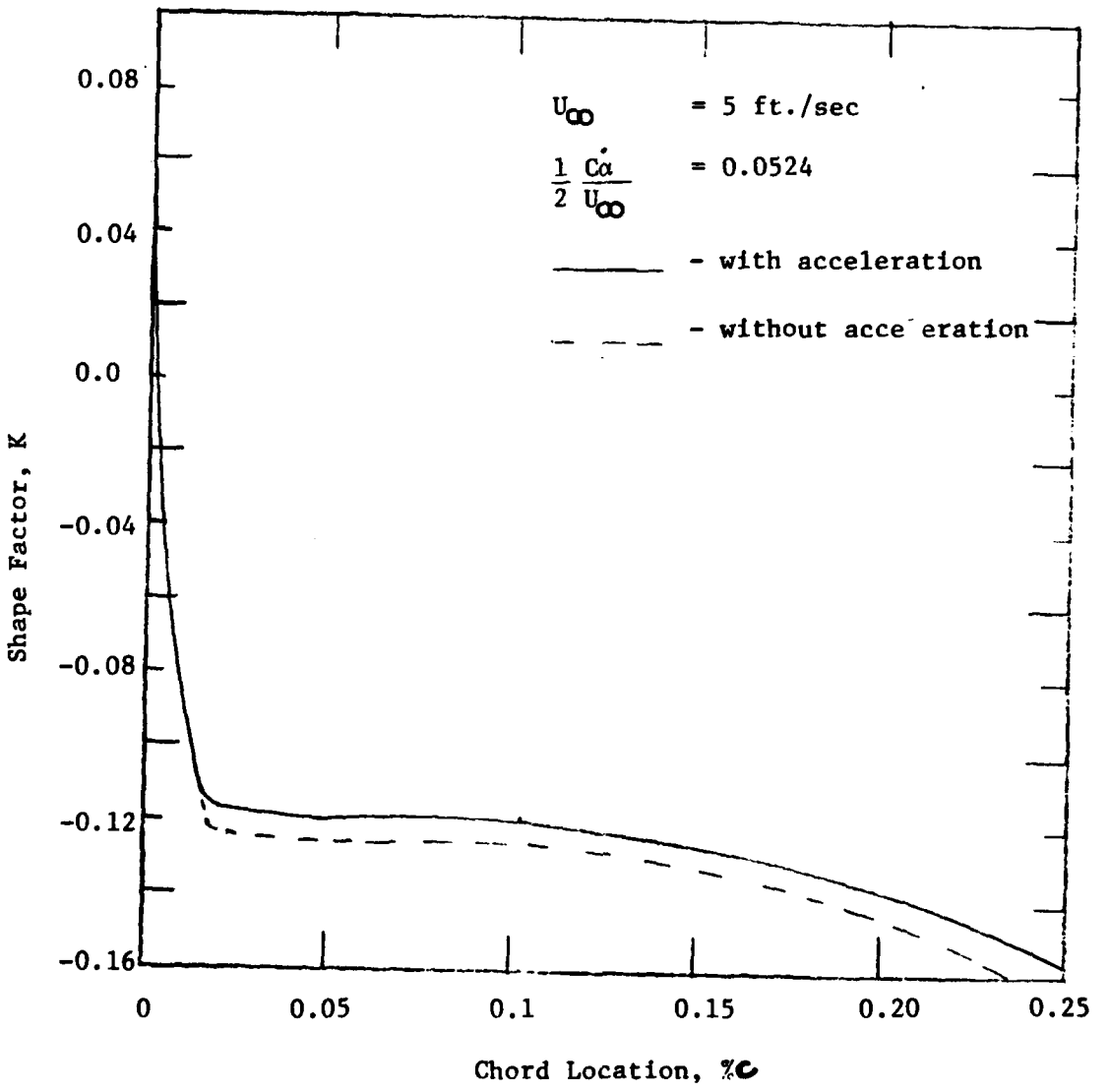

Figure 10. Effect of Acceleration Due to Pitching on Boundary Layer Shape Parameter

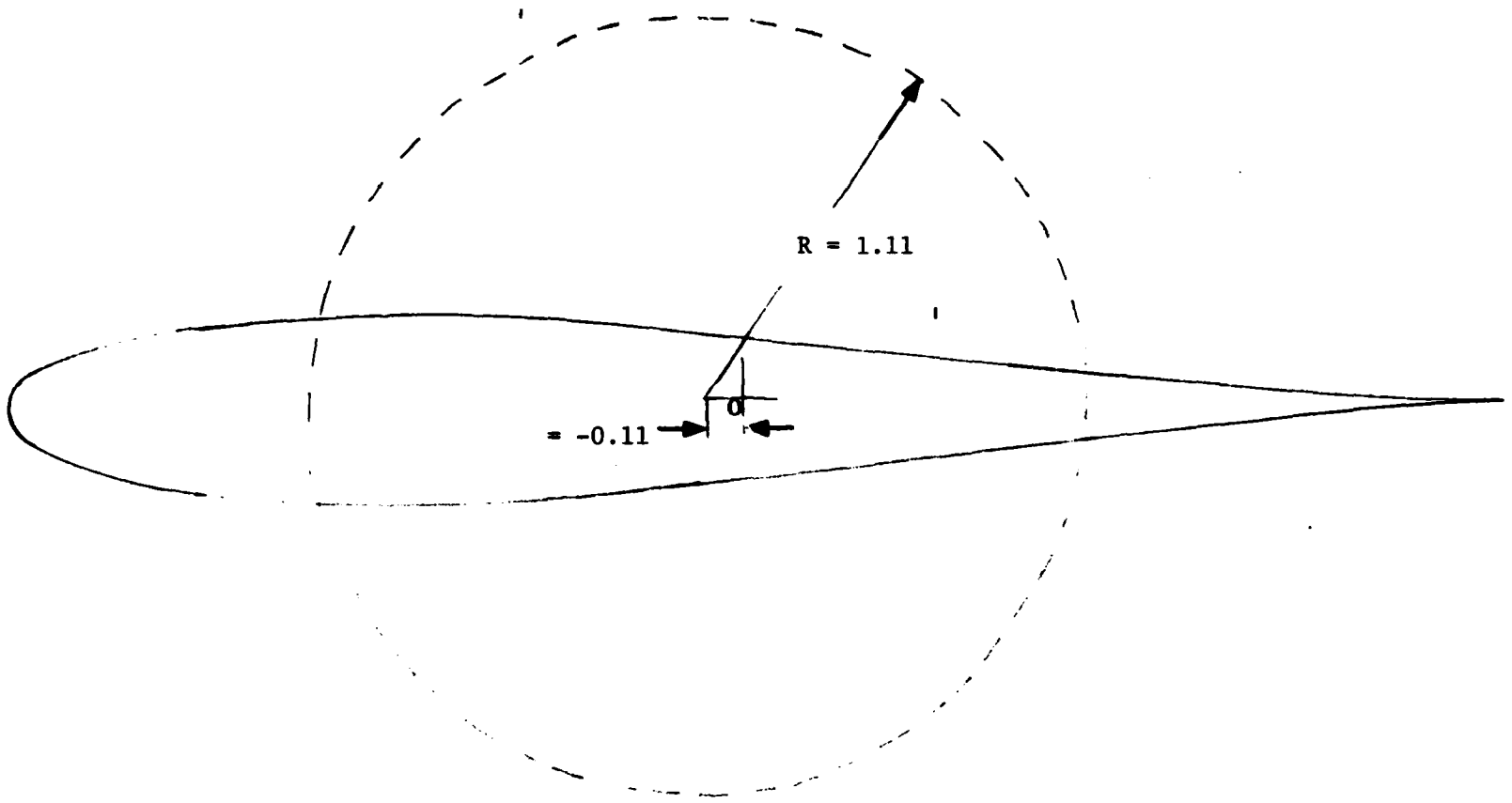

Figure 11. Joukowski Airfoil and Reference Circle

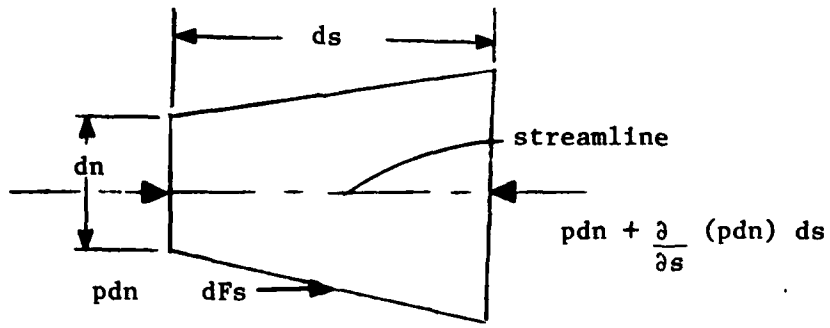

a. Forces

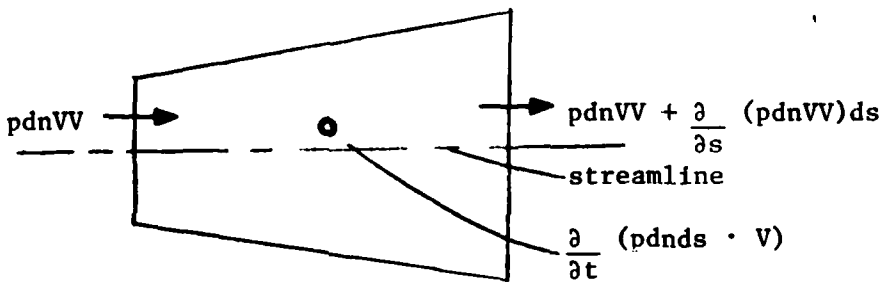

b. Momentum into and out of a Control Volume Element

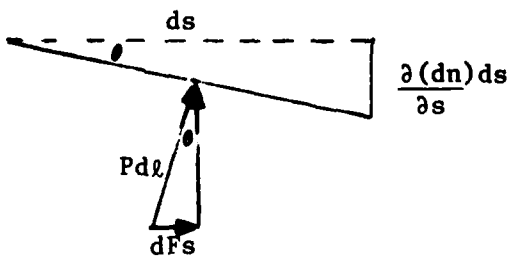

c. Depiction of dFs

Figure 12. Fluid Element Along a Streamline

Appendix A

Throughout this study, many references are made to the inviscid flow velocity, or the velocity of the potential flow, and so on. In this appendix, it is shown how to derive that velocity by using complex potential flow theory.

Complex Flow Velocity

The complex velocity about a body is the first derivative of the complex flow potential that describes the flow:

$$w(z) = dF(z)/dz \quad \text{(Ref. 5)} \tag{A1}$$

where $w(z)$ = the complex velocity and

$F(z)$ = the complex flow potential

Now, to obtain the expression for the complex flow velocity for the problem of this study, i.e. flow about an airfoil, it is necessary to first find the velocity about a cylinder (that will transform into the desired airfoil), and then transform that velocity via the Joukowski transformation into the corresponding velocity about the airfoil. The describing equation for the complex potential flow about a cylinder is a uniform stream at angle of attack is:

$$F(z) = U_\infty (z + R^2/z) + i (\Gamma \ln z)/2\pi \tag{A2}$$

Then, the corresponding velocity is:

$$w(z) = U_\infty (1 - R^2/z^2) + i \Gamma/2\pi z \tag{A3}$$

The Kutta condition that air flows smoothly off the trailing edge (Ref. 6:34) dictates the amount of circulation required:

$$\Gamma = 4 \; U_\infty R \sin \alpha \tag{A4}$$

for symmetric airfoils (Ref. 5). Substituting (A4) into (A3):

$$w(z) = U_\infty (1 - R^2/z^2) + i (2 U_\infty R \sin \alpha)/z \tag{A5}$$

which described the velocity w at any point z(x,iy) on a cylinder of radius R, with its center at the origin.

The advantage to using complex potential flow theory is that flows due to different phenomena can be superimposed to form one flow. In the problem of this study, it is desired to simulate uniform flow about a cylinder at some angle of attack in two-dimensional space.

To generate flow about a cylinder, a doublet must be used. Flow at angle of attack (that produces lift) requires circulation, which is provided via the use of a vortex. The describing functions of each of these in complex potential flow theory are:

Uniform stream:	$U_\infty \cdot z$	(A6.a)
Doublet:	$U_\infty \cdot R^2/z$	(A6.b)
Vortex:	$i\ (\Gamma \ln z)/2\pi$	(A6.c)

(Ref. 7:449)

Now, to describe the flow about a corresponding airfoil, use:

$$|w(\zeta)| = |w(z)| \ / \ |d\zeta/dz| \tag{A7}$$

where

$w(\zeta)$ = flow about the airfoil (or body)

$w(z)$ = flow about the cylinder

$d\zeta/dz$ = the derivative of the function that transforms the cylinder to the airfoil.

The general transformation from a cylinder to a flat plate (airfoil of zero thickness) is:

$$\zeta = z + R^2/z \tag{A8}$$

So that

$$\frac{d\zeta}{dz} = 1 - R^2/z^2$$

To generate an airfoil with thickness, like that which is being used for this study, the center of the circle must be offset along the real axis, into the flow so as to generate an airfoil with thickness with the proper orientation:

$$z' = z + X_o$$

where X_o = the amount of offset. Thus, the transformation is:

$$\frac{d\zeta}{dz} = 1 - R^2/z'^2$$

This formulation of how to compute the velocity at a point $\zeta(\xi, i\eta)$ on the airfoil has been programmed as a subroutine in the computer program developed for this study (see Appendix E).

Joukowski Airfoil Development

The theory developed in this study is applied to a Joukowski airfoil to test the validity of that theory. As mentioned earlier, a Joukowski airfoil is used because the potential flow about a Joukowski airfoil is easily described without having to use various other complex transformations although they can be used and applied.

The development of a Joukowski airfoil has its roots in complex variable theory. It is created by transforming a circular cylinder in one plane through a transformation function into the plane of the airfoil (Ref. 12:237 and Ref. 5). Although arguments against Joukowski airfoils exist primarily because of its cusped trailing edge, it is used here because its leading edge characteristics and geometry closely parallel those of several practical airfoils.

To map a Joukowski airfoil, either a graphical or a mathematical/computer solution can be used. In this study, a computer solution is chosen. As stated, a Joukowski airfoil is created through a circular

cylinder that will map into the desired airfoil. In this study, it was desired to simulate a NACA 1102 airfoil leading quarter chord. Through trial and error, it was found that an 11% thick Joukowski airfoil best did this.

Thus, to generate a symmetric airfoil, a cylinder was offset from the origin into the flow and is described by a series of points:

$$z(x, iy) = R \exp (i \cdot \theta) + \mu, \tag{A9}$$

where R is the radius of the cylinder, θ is an angle that locates a point (x, iy) on a cylinder of radius R, and μ is the distance that the origin of the cylinder is offset into the flow. μ can be either totally real to generate thickness only or totally imaginary to generate a flat plate cambered airfoil or complex to generate an airfoil with both thickness and camber.

Now, to create the airfoil, the circular cylinder was passed through the transformation function

$$\zeta(\xi, i\eta) = x(x, iy) + \frac{R^2}{z(x, iy)}, \tag{A8}$$

where $\zeta(\xi, i\eta)$ describes the points of the airfoil.

A plot of the airfoil is given in Fig. 11.

Euler's Equation of Motion

To develop Euler's equation of motion in unsteady flow, use is made of a fluid element along a streamline (Fig. 12). The sum of the forces along the streamline are:

$$pdn - \left(pdn + \frac{\partial(pdn)}{\partial s} ds\right) + dF_s$$

where

p = pressure

dn = the differential length normal to the streamline

ds = differential length along the streamline

dF_s = force on the side of the element in the direction of the streamline.

To find F_s as a function of pressure, look at the sidewall geometry (Fig. 12c). It is evident from the geometry that:

$$dF_s = pdl \sin\theta$$

But,

$$\sin\theta = \frac{\partial(dn)}{\partial s} ds \cdot \frac{1}{dl}$$

$$dF_s = p \frac{\partial(dn)}{\partial s} ds \;;$$

$\therefore$ the sum of the forces $= - \frac{\partial(pdn)}{\partial s} ds + p \frac{\partial(dn)}{\partial s} ds$

But,

$$\frac{\partial(pdn)}{\partial s} = dn \frac{\partial p}{\partial s} + p \frac{\partial(dn)}{\partial s};$$

$\therefore$ the sum of the forces $= - \frac{\partial p}{\partial s} dnds$ (A10)

Now, the momentum flux through this fluid element is (Fig. 12b):

$$\dot{M}_o - \dot{M}_i + \frac{\partial}{\partial t} (M_{cv})$$

which is equal to:

$$pdnVV + \frac{\partial}{\partial s} (pdnVV) ds - pdnVV + \frac{\partial}{\partial t} (pdndsV)$$

For incompressible flow,

$$\frac{\partial\rho}{\partial s} = \frac{\partial\rho}{\partial t} = 0;$$

$\therefore$ the mass flux is:

$$\rho dnds \left(\frac{\partial}{\partial s} (V^2) + \frac{\partial V}{\partial t}\right)$$

Assuming dn and ds to be independent of each other, the mass flux is equal to:

$$\rho dnds\left(V\frac{\partial V}{\partial s} + \frac{\partial V}{\partial t}\right) \tag{A11}$$

Equating (A10) and (A11) through the momentum principle:

$$\rho dnds \left(V\frac{\partial V}{\partial s} + \frac{\partial V}{\partial t}\right) = - \frac{\partial p}{\partial s} dnds. \tag{A12}$$

Dividing by $\rho dnds$, equation (A12) becomes:

$$V\frac{\partial V}{\partial s} + \frac{\partial V}{\partial t} = - \frac{1}{\rho} \frac{\partial p}{\partial s} , \tag{A13}$$

the Euler equation of motion for unsteady flow.

Appendix B

The momentum-integral equation for boundary layer in steady flow is reproduced here. Those not familiar with the derivation of this equation as it is done here may wish to review it before reading Chapter III.

The momentum-integral equation is developed by deriving the continuity and momentum equations for a fluid element in the boundary layer and then integrating the momentum equation through the boundary layer.

M-I Equation for Steady flow

The Continuity Equation. In words, the continuity equation states that the net rate of mass flow out of a control volume is equal to the time rate of loss of mass within that control volume (Ref. 2:10).

Referring to Fig. 7, this gives

$$\dot{m}_{out} = \int_o^h \rho u dy + \frac{\partial}{\partial x}\left(\int_o^h \rho u dy\right) dx + \dot{m}_{o_{top}}$$

$$\dot{m}_{in} = \int_o^h \rho u dy$$

Notice that there is no mass flow rate into the control volume element from the body which satisfies the "no penetration" condition.

The time rate of loss of mass in steady flow is zero; therefore, the continuity equation for steady flow becomes:

$$\frac{\partial}{\partial x} \int_o^h (u dy) dx + \dot{m}_{o_{top}} = 0$$

Momentum Principle

The momentum principle states that the sum of the forces acting on the fluid in a control volume is equal to the net rate of transport of momentum out of the control volume (Ref. 2:11).

Referring to Fig. 8, then the x-component of the momentum equation may be found by finding the sum of the forces in the x-direction

$$\Sigma F_x = -\tau_w dx + \int_o^h p dy - \int_o^h p dy - \frac{\partial}{\partial x}\left(\int_o^h p dy\right) dx,$$

and equating it to the momentum terms:

$$\int_o^h \rho u u dy + \frac{\partial}{\partial x}\left(\int_o^h \rho u u dy\right) dx - \int_o^h \rho u u dy + \dot{m}_{o_{top}} \cdot Ue,$$

such that

$$\frac{\partial}{\partial x}\left(\int_o^h \rho u u dy\right) dy + \dot{m}_{o_{top}} \cdot Ue = -\tau_w dx - \frac{\partial}{\partial x}\left(\int_o^h p dy\right) dx. \qquad \text{(B2)}$$

$\dot{m}_{o_{top}}$ can be replaced with its solution obtained in the development of the continuity equation

$$\dot{m}_{o_{top}} = -\frac{\partial}{\partial x}\left(\int_o^h \rho u dy\right) dx, \qquad \text{(B1)}$$

so that the momentum equation becomes

$$\frac{\partial}{\partial x}\left(\int_o^h \rho u u dy\right) dx - Ue \cdot \frac{\partial}{\partial x}\left(\int_o^h \rho u dy\right) dx = -\tau_w dx - \frac{\partial}{\partial x}\left(\int_o^h p dy\right) dx.$$

All the integrations are with respect to y. Since x and y are independent functions, the partial derivatives can be pulled inside the integrals:

$$\int_o^h \frac{\partial}{\partial x}(\rho u u) dy dx - Ue \cdot \int_o^h \frac{\partial}{\partial x}(\rho u) dy dx = -\tau_w dx - \int_o^h \frac{\partial}{\partial x}(p) dy dx$$

From the boundary layer assumptions, it is known that $\partial p/\partial y$ is zero. Since this is true, and since the problem is two-dimensional, the pressure gradient in the x-direction is the only pressure gradient, and the partial derivative of pressure can be replaced by a total (not substantial) derivative:

$$\int_o^h \frac{\partial}{\partial x}(\rho uu)dydx - Ue \cdot \int_o^h \frac{\partial}{\partial x}(\rho u)dydx = -\tau_w dx - \int_o^h \frac{dp}{dx}dydx \qquad \text{(B3)}$$

If the fluid is further restricted to incompressible flow, then ρ can be divided through. Also, divide through by the common dx term:

$$\int_o^h \frac{\partial}{\partial x}(uu)dy - Ue \cdot \int_o^h \frac{\partial}{\partial x}(u)dy = -\frac{\tau_w}{\rho} - \frac{1}{\rho}\int_o^h \frac{dp}{dx}$$

Now, Euler's equation for steady flow can be used to substitute into equation (B3) for the pressure gradient:

$$-\frac{1}{\rho}\frac{dp}{dx} = Ue\frac{dUe}{dx} \qquad \text{(B4)}$$

$$\int_o^h \frac{\partial}{\partial x}(uu)dy - Ue \cdot \int_o^h \frac{\partial}{\partial x}udy = -\frac{\tau_w}{\rho} + \int_o^h Ue\frac{dUe}{dx}dy$$

Rearranging terms:

$$-\int_o^h \frac{\partial uu}{\partial x}dy + Ue\int_o^h \frac{\partial u}{\partial x}dy + \int_o^h Ue\frac{dUe}{dx} = \frac{\tau_w}{\rho} \qquad \text{(B5)}$$

Notice that the second term looks like part of

$$\int_o^h \frac{\partial(uUe)}{\partial x}dy,$$

which is a <u>form</u> that is identical to the first term. Expanding this term out

$$\int_o^h \frac{\partial(uUe)}{\partial x}dy = \int_o^h u\frac{\partial Ue}{\partial x}dy + \int_o^h Ue\frac{\partial u}{\partial x}dy. \qquad \text{(B6)}$$

The second term on the right hand side is the second term in equation (B5). Thus, if the first term on the right hand side of equation (B6) is both added and subtracted from equation (B5) (hence adding zero to the equation), it looks like

$$-\int_o^h \frac{\partial(uu)}{\partial x}dy + Ue \cdot \int_o^h \frac{\partial u}{\partial x}\,dy + \int_o^h u\,\frac{dUe}{dx}\,dy + \int_o^h Ue\,\frac{dUe}{dx}\,dy - \int_o^h u\,\frac{dUe}{dx}\,dy = \frac{\tau_w}{\rho} \qquad \text{(B7)}$$

Combining the second and third terms of equation (B7) to get the term of the left hand side of equation (B6) gives

$$-\int_o^h \frac{\partial}{\partial x}(uu)dy + \int_o^h \frac{\partial}{\partial x}(uUe)dy + \int_o^h Ue\,\frac{dUe}{dx}\,dy - \int_o^h u\,\frac{dUe}{dx}\,dy = \frac{\tau_w}{\rho}. \qquad \text{(B8)}$$

The velocity gradient at the edge of the boundary layer. dUe/dx is a function of x, along the direction of flow, and is independent of the height away from the body. Thus, this term can be brought outside the integral. In addition, the first two terms and the second two terms are similar and can now be combined:

$$\int_o^h \frac{\partial}{\partial x}(uUe - uu)dy + \frac{dUe}{dx}\int_o^h (Ue - u)dy = \frac{\tau_w}{\rho}$$

Bring the partial derivative outside the integral and rearrange the terms to get

$$\frac{\partial}{\partial x}\,Ue^2 \int_o^h \frac{u}{Ue}\left(1 - \frac{u}{Ue}\right)dy + Ue\,\frac{dUe}{dx}\int_o^h \left(1 - \frac{u}{Ue}\right)dy = \frac{\tau_w}{\rho}\,, \qquad \text{(B9)}$$

which is the momentum-integral equation for boundary layers in steady flow.

Appendix C

The von Karman-Pohlhausen integral method for steady flow is reproduced here again for those readers not familiar with its development.

Method of von Karman and Pohlhausen - Steady State

The momentum-integral equation for steady flow is:

$$\frac{\partial}{\partial x} Ue^2 \int_o^h \left(\frac{u}{Ue}\right)\left(1 - \frac{u}{Ue}\right) dy + Ue \frac{dUe}{dx} \int_o^h \left(1 - \frac{u}{Ue}\right) dy = \frac{\tau_w}{\rho} \qquad \text{(B9) and (C1)}$$

Two parameters relating to the boundary layer thickness are now introduced:

$$\delta_1 = \int_o^h \left(1 - \frac{u}{Ue}\right) dy \qquad \text{(C2)}$$

$$\delta_2 = \int_o^h \frac{u}{Ue} \left(1 - \frac{u}{Ue}\right) dy \qquad \text{(C3)}$$

Equation (C2) represents the displacement thickness; equation (C3) represents the momentum thickness (see Fig. 4). Substituting into the momentum-integral equation:

$$\frac{\partial}{\partial x} (Ue^2 \delta_2) + Ue\delta_1 \frac{dUe}{dx} = \frac{\tau_w}{\rho} \qquad \text{(C4)}$$

Expanding out the first term:

$$2Ue\delta_2 \frac{dUe}{dx} + Ue^2 \frac{d\delta_2}{dx} + Ue\delta_1 \frac{dUe}{dx} = \frac{\tau_w}{\rho}$$

or

$$(2\delta_2 + \delta_1)\, Ue \frac{dUe}{dx} + Ue^2 \frac{d\delta_2}{dx} = \frac{\tau_w}{\rho} \qquad \text{(C5)}$$

For the boundary layer to be computed, then something must be known about $\delta 1$ and $\delta 2$. However, these are in terms of an as yet

unspecified velocity profile, u/Ue. The velocity profile must satisfy two constraints:

1. The order of the velocity equation must be in accord with the number of boundary conditions.

2. The velocity profile must allow for an inflexion point, since the flow will be with a pressure gradient (Ref. 3:207).

The boundary conditions available are:

$$y = 0 \qquad u = 0 \tag{C6.a}$$

$$\nu \partial^2 u/\partial y^2 = -\ Ue\ dUe/dx \tag{C6.b}$$

$$y = \delta \qquad u = Ue \tag{C6.c}$$

$$\partial u/\partial y = 0 \tag{C6.d}$$

$$\partial^2 u/\partial y^2 = 0 \tag{C6.e}$$

The existence of five boundary conditions allows for the solution of five constants. In other words, a 4th order polynomial is required for the velocity profile. The form of the velocity profile is:

$$\frac{u}{Ue} = A + B\eta + C\eta^2 + D\eta^3 + E\eta^4$$

Applying (C6.a):

$$A = 0 \tag{C7.a}$$

Applying (C6.c):

$$1 = B + C + D + E \tag{C7.b}$$

Applying (C6.d):

$$0 = B + 2C + 3D + 4E \tag{C7.c}$$

Applying (C6.e):

$$0 = 2C + 6D + 12E \tag{C7.d}$$

Applying (C6.b):

$$\frac{\partial^6 (u/Ue)}{\partial (y/\delta)} = B + 2C\eta + 3D\eta^2 + 4E\eta^3$$

$$y = 0$$

$$\frac{\partial^2 (u/Ue)}{\partial (y/\delta)^2} = 2C + 6D\eta + 12E\eta^2 \Big|_{\eta = 0}$$

$$2C = -\frac{\delta^2}{\nu} \frac{dUe}{dx} \qquad \text{(C7.e)}$$

At this point, a dimensionless parameter, Λ, is introduced:

$$\Lambda \equiv \frac{\delta^2}{\nu} \frac{dUe}{dx} \qquad \text{(C8)}$$

Substituting (C8) into (C7.e) and subsequently solving equations (C7.a) through (C7.d):

$$A = 0$$

$$B = 2 + \Lambda/6$$

$$C = \quad - \Lambda/2$$

$$D = -2 + \Lambda/2$$

$$E = 1 - \Lambda/6$$

For details on this solution, see Appendix D.

The velocity profile is now:

$$\frac{u}{Ue} = (2\eta - 2\eta^3 + \eta^4) + \Lambda/6\ (\eta - 3\eta^2 + 3\eta^3 - \eta^4)$$

and δ_1 and δ_2 can now be solved:

$$\frac{\delta_1}{\delta} = \frac{1}{\delta} \int_0^1 (1 - \frac{u}{Ue})^{dy}$$

For $y > \delta$, $u = Ue$ by definition of the boundary layer, and integration beyond $y = \delta$ makes no sense. Therefore:

$$\frac{\delta_1}{\delta} = \frac{1}{\delta} \int_0^1 (1 - \frac{u}{Ue})^{dy}$$

Previously, η was defined as y/δ. Introduce this into the displacement thickness, and redefine the limits of integration

$$\frac{\delta_1}{\delta} = \int_0^1 (1 - \frac{u}{Ue})^{d\eta};$$

Substituting for u/Ue, this gives:

$$\frac{\delta_1}{\delta} = \int_0^1 \left[1 - (2\eta - 2\eta^3 + \eta^4) + \Lambda/6\ (\eta - 3\eta^2 + 3\eta^3 - \eta^4)\right] d\eta;$$

Integrating this out and evaluating at the limits yields

$$\frac{\delta_1}{\delta} = \frac{3}{10} - \frac{\Lambda}{120} \tag{C9}$$

Similarly, for the momentum thickness,

$$\frac{\delta_2}{\delta} = \int_0^1 \left[(2\eta - 2\eta^3 + \eta^4) + \frac{\Lambda}{6}\ (\eta - 3\eta^2 + 3\eta^3 - \eta^4)\right].$$

$$\left[1 - (2\eta - 2\eta^3 + \eta^4)\ \frac{\Lambda}{6}\ (\eta - 3\eta^2 + 3\eta^3 - \eta^4)\right] d\eta.$$

Integrating this out and evaluating this at the limits

$$\frac{\delta_2}{\delta} = \frac{37}{315} - \frac{\Lambda}{945} - \frac{\Lambda^2}{9072}\ . \tag{C10}$$

For details of the integration, see Appendix D.

The shear stress at the wall, τ_w, can be written as:

$$\tau_w = \mu\ \frac{Ue}{\delta}\ \frac{\partial(u/Ue)}{\partial(y/\delta)}$$

$$\frac{\tau_w}{\mu Ue} = \left.\frac{\partial(u/Ue)}{\partial(y/\delta)}\right| = 2 + \quad \Lambda/6. \tag{C11}$$

This also gives the separation criteria, since separation is defined as when the shear stress at the wall becomes zero. Applying this definition gives

$$\frac{\tau_w \delta}{\mu Ue} = 2 + \frac{\Lambda}{6} = 0.$$

$$\Lambda = -12, \tag{C12}$$

the criteria for flow separation.

Rearrange the momentum-integral equation into a more workable form:

$$(2\delta_2 + \delta_1)Ue\ \frac{dUe}{dx} + Ue^2\ \frac{d\delta_2}{dx} = \frac{\tau_w}{\rho} \tag{C5}$$

Multiply by δ_2 and divide by ν:

$$\frac{\delta_2^2}{\nu}(2 + \delta_1/\delta_2)\, Ue \frac{dUe}{dx} + Ue^2 \frac{\delta_2\delta_2'}{\nu} = \frac{\tau_w\delta_2}{\nu}$$

divide by Ue:

$$\left(2 + \frac{\delta_1}{\delta_2}\right) \frac{\delta_2^2}{\nu} \frac{dUe}{dx} + Ue \frac{\delta_2\delta_2'}{\nu} = \frac{\tau_w\delta_2}{Ue\nu} \tag{C13}$$

Another dimensionless parameter is now introduced:

$$K \equiv z\, dUe/dx \tag{C14.a}$$

$$K \equiv \frac{\delta_2^2}{\nu}\, dUe/dx \tag{C14.b}$$

In equation (C13), the right hand side is:

$$\frac{\tau_w\delta_2}{\mu Ue} = \frac{\tau_w\delta}{\mu Ue} \cdot \frac{\delta_2}{\delta}$$

which can be expressed strictly as a function of Λ:

$$\frac{\tau_w\delta_2}{\mu Ue} = (2 + \Lambda/6)\left(\frac{37}{315} - \frac{\Lambda}{945} - \frac{\Lambda^2}{9072}\right) \tag{C15.a}$$

which, for the Pohlhausen technique, is defined as $f_2(K)$.

Similarly:

$$K = \Lambda\left(\frac{\delta_2}{\delta}\right)^2$$

$$= \left(\frac{37}{315} - \frac{\Lambda}{945} - \frac{\Lambda^2}{9072}\right)^2\Lambda \tag{C15.b}$$

Finally:

$$\frac{\delta_1}{\delta_2} = \frac{\delta_1}{\delta} \cdot \frac{\delta}{\delta_2} = \left(\frac{3}{10} - \frac{\Lambda}{120}\right)\left(\frac{37}{315} - \frac{\Lambda}{120} - \frac{\Lambda^2}{9072}\right)^{-1} \tag{C16}$$

which, again, for the Pohlhausen integration is defined as $f_1(K)$. Thus, the momentum-integral equation becomes:

$$\left[2 + f_1(K)\right] K + \frac{Ue\delta_2\delta_2'}{\nu} = f_2(K) \tag{C17}$$

Now:

$$\frac{Ue\delta_2\delta_2'}{\nu} = \frac{1}{2}\frac{Ue}{\nu}\frac{d(\delta_2^2)}{dx}$$

$$\frac{Ue\delta_2\delta_2}{\nu} = \frac{1}{2}\, Ue\, \frac{d(\delta_2{}^2/\nu)}{dx}$$

$$\frac{Ue\delta_2\delta_2}{\nu} = \frac{1}{2}\, Ue\, \frac{dz}{dx} \qquad \text{(C18)}$$

Substituting (C18) into (C17) gives

$$\left[2 + f_1(K)\right] K + \frac{1}{2}\, Ue\, \frac{dz}{dx} = f_2(K),$$

or

$$Ue\, \frac{dz}{dx} = 2f_2(K) - 2Kf_1(K) - 4K \qquad \text{(C19)}$$

Now, the right hand side of equation (C19) can be defined as

$$2f_2(K) - 2Kf_1(K) - 4K \equiv F(K), \qquad \text{(C20)}$$

so substitution of (C20) into (C19) yields

$$\frac{dz}{dx} = \frac{F(K)}{Ue} \qquad \text{(C21.a)}$$

$$z = K/Ue' \qquad \text{(C14.a and C21.b)}$$

which are the only two equations required to solve the boundary layer by the method of von Karman and Pohlhausen

The integration procedure begins at the stagnation point of the airfoil. Recall that at the stagnation condition, Ue = 0, to maintain a finite dz/dx, F(K) = 0. Solving equation (C20) with appropriate substitutions for $f_1(K)$, $f_2(K)$, and K, it is found that:

$$\Lambda_o = 7.052 \qquad \text{(C22.a)}$$

$$K_o = 0.0770 \qquad \text{(C22.b)}$$

For details on this, see Appendix D.

Thus,

$$z_o = 0.0770/U'_o$$

and

$$dz/dx\Big|_o = \frac{0}{0}$$

Using the limit (Ref. 3:211):

$$dz/dx\Big|_o = -0.0652\ U''_o/(U'_o)^2$$

Now, to complete the discussion on the Pohlhausen integration, the steps to integrate the boundary layer are:

1. Determine the velocity and velocity gradient dUe/dz from the potential flow solution for the shape of interest (see Appendix A) in addition to the arc length segments along the body.

2. Knowing z_o and dz/dx,

$$z_1 = z_o + \frac{dz}{dx}\Big|_o \cdot dx,$$

where dx is an increment of arc length along the airfoil.

3. Compute a new value of K from equation (C21.b). At this point, the value of Λ can be backed out from equation (C15.b) to determine flow attachment or separation; however, an easier way to determine flow separation (and the method used for this study) is to find the value of K that corresponds to $\Lambda = -12$, and use this as the flow separation criteria. The value is K = -1567 (Ref. 3:212).

4. F(K) is determined either by:

   a. Knowing Λ and solving equation (C19), or

   b. Approximate F(K) vs K by a linear approximation:

$$F(K) = a - bK \qquad \text{(C23)}$$

$$\text{with} \quad a = .47$$

$$b = 6 \qquad \text{(Ref. 3:213)}$$

5. Knowing F(K) from the linear approximation and Ue from the potential flow solution, determine the new value of dz/dx.

6. Compute a new z by:

$$z_{i+1} = z_i + \frac{dz}{dx}\Big|_i \cdot dx_i$$

7. For this study, repeat steps 3 through 6 until:

a) The 1/4-chord point is reached. Check K against the separation criteria. If the flow is not separated ($K = -0.1567$), select a higher angle of attack, and repeat until flow separation at the 1/4-chord is indicated.

b) Then stop the computations and record the steady state stall angle.

Appendix D

Solution of the Constants in the Velocity Equation

The three equations that remain to be solved are:

$$B + 2C + 3D + 4E = 0$$

$$2C + 6D + 12E = 0$$

$$B + C + D + E = 1.$$

Substituting $C = -\Lambda/2$, and setting up an augmented matrix:

$$\left[\begin{array}{ccc|cc} 1 & 3 & 4 & 0 & \Lambda \\ 0 & 6 & 12 & 0 & \Lambda \\ 1 & 1 & 1 & 1 & \Lambda/2 \end{array}\right]$$

Now performing elementary row operations:

Row 2 ÷ by 6:

$$\left[\begin{array}{ccc|cc} 1 & 3 & 4 & 0 & \Lambda \\ 0 & 1 & 2 & 0 & \Lambda/6 \\ 1 & 1 & 1 & 1 & \Lambda/2 \end{array}\right]$$

Row 3 - row 1 + 2 · row 2:

$$\left[\begin{array}{ccc|cc} 1 & 3 & 4 & 0 & \Lambda \\ 0 & 1 & 2 & 0 & \Lambda/6 \\ 0 & 0 & 1 & 1 & -\Lambda/6 \end{array}\right]$$

Row 1 - 4 · row 3; row 2 - 2 · row 3:

$$\left[\begin{array}{ccc|c} 1 & 3 & 0 & -4 + 5/3 \cdot \Lambda \\ 0 & 1 & 0 & -2 + \Lambda/2 \\ 0 & 0 & 1 & 1 - \Lambda/6 \end{array}\right]$$

Row 1 - 3 · row 2:

$$\left[\begin{array}{ccc|c} 1 & 0 & 0 & 2 + \Lambda/6 \\ 0 & 1 & 0 & -2 + \Lambda/2 \\ 0 & 0 & 1 & 1 - \Lambda/6 \end{array}\right]$$

Thus, the constants are:

$$A = 0$$

$$B = 2 + \Lambda/6$$

$$C = \quad - \Lambda/2$$

$$D = -2 + \Lambda/2$$

$$E = 1 - \Lambda/6$$

<u>Solution of δ_1/δ:</u>

$$\frac{\delta_1}{\delta} = \int_0^1 \left(1 - \frac{u}{Ue}\right) d\eta$$

$$= \int_0^1 \left[1 - \left(2 + \frac{\Lambda}{6}\right)\eta + \left(-\frac{\Lambda}{2}\right)\eta^2 + \left(-2 + \frac{\Lambda}{2}\right)\eta^3 + \left(1 - \frac{\Lambda}{6}\right)\eta^4\right] d\eta$$

$$= \eta - \left(2 + \frac{\Lambda}{6}\right)\frac{\eta^2}{2} - \left(-\frac{\Lambda}{2}\right)\frac{\eta^3}{3} - \left(-2 + \frac{\Lambda}{2}\right)\frac{\eta^4}{4} - \left(1 - \frac{\Lambda}{6}\right)\frac{\eta^5}{5} \Bigg|_0^1$$

$$= 1 - \left(1 + \frac{\Lambda}{12}\right) - \left(-\frac{\Lambda}{6}\right) - \left(-\frac{1}{2} + \frac{\Lambda}{8}\right) - \left(\frac{1}{5} - \frac{\Lambda}{30}\right)$$

$$= \left(1 - 1 + \frac{1}{2} - \frac{1}{5}\right) + \Lambda\left(-\frac{1}{12} + \frac{1}{6} - \frac{1}{8} + \frac{1}{30}\right)$$

$$\frac{\delta_1}{\delta} = \frac{3}{10} - \frac{\Lambda}{120}$$

<u>Solution of δ_2/δ:</u>

$$\frac{\delta_2}{\delta} = \int_0^1 \frac{u}{Ue}\left(1 - \frac{u}{Ue}\right) d\eta.$$

It is more convenient to solve δ_2/δ in terms of the constants A, B, C, D, and G, and then substitute for their values later.

$$\frac{\delta_2}{\delta} = \int_0^1 \left[(B\eta + C\eta^2 + D\eta^3 + E\eta^4)(1 - B\eta - C\eta^2 - D\eta^3 - E\eta^4)\right] d\eta$$

$$\frac{\delta_2}{\delta} = \int_0^1 \left[B\eta + (-B^2 + C)\eta^2 + (-2BC + D)\eta^3 + (-2BC - C^2 + E)\eta^4\right] d\eta$$

$$= \left[(-2BE - 2CD)\eta^5 + (-2CE - D^2)\eta^6 + (-2DE)\eta^7 + (-E^2)\eta^8\right] d\eta$$

$$= \frac{B\eta^2}{2} + \frac{(-B2 + C)}{3}\eta^3 + \frac{(-2BC + D)}{4}\eta^4 + \frac{(-2BD - C^2 + E)}{5}\eta^5$$

$$+ \frac{(-2BE - 2CD)}{6}\eta^6 + \frac{(-2CE - D^2)}{7}\eta^7 + \frac{-2DE}{8}\eta^8 + \frac{-E^2}{9}\eta^9 \Bigg|_0^1$$

Substituting:

$$B = 2 + \Lambda/6$$

$$C = \quad - \Lambda/2$$

$$D = -2 + \Lambda/2$$

$$E = 1 - \Lambda/6$$

$$\frac{\delta 2}{\delta} = .1175 - .001\Lambda \quad - .00011\Lambda^2$$

$$= \frac{37}{315} - \frac{\Lambda}{945} - \frac{\Lambda^2}{9072}$$

<u>Solution of Stagnation Condition for Λ.</u>

At the stagnation point, F(K) = 0 so that dz/dx at that point is finite, since

$$\frac{dz}{dx}\Big| = \frac{F(K)}{U_o}, \text{ and } U_o = 0$$

$$F(K) = 2\left(\frac{37}{315} - \frac{\Lambda}{945} - \frac{\Lambda^2}{9072}\right)\left[2 - \frac{116}{315}\Lambda + \left(\frac{2}{945} + \frac{1}{120}\right)\Lambda^2 + \frac{2}{9072}\Lambda^3\right]$$

(Ref. 3:210)

Setting this to zero:

$$\left(\frac{37}{315} - \frac{\Lambda}{945} - \frac{\Lambda^2}{9072}\right)\left[2 - \frac{116}{315}\Lambda + \left(\frac{2}{945} + \frac{1}{120}\right)\Lambda^2 + \frac{2}{9072}\Lambda^3\right] = 0. \qquad \text{(D1)}$$

This can be expanded out, and solved by mathematical tools, or we can try different values of Λ until equation (1) is satisfied. This gives:

$$\Lambda_o = 7.052;$$

and

$$K_o = 0.0770.$$

```
      PROGRAM POHL2
C
C     PROGRAM BY CAPT R G DICKE  JR
C     AF INSTITUTE OF TECHNOLOGY
C     GAE-820
C
      COMPLEX CMPLX,EI,Z,DZETA,
      EI = (0.,1.)
      RADIUS = 1.11
      AMU = -.11
      READ*,ALPHA,ADOT1
      UINF = 5.0
      ALPHI = ALPHA
      CON = 3.1415927/180.
      VNU = 1.546E-04
      THETA = 180.
      TIME = 0.0
      PITCH = ADOT1 * CON * 0.5/UINF
      CALL DS(180.,RADIUS,CON,AMU,XLE,YLE)
      CALL DS(0.0,RADIUS,CON,AMU,XTE,YTE)
      XLE = ABS(XLE)
      CHORD = XLE + XTE
C
C
      K = 10000
      K1 = K + 1
      K2 = (ALPHA + 150)*100 + K
C
      WRITE(6,30)UINF
      WRITE(6,40)ALPHA
      WRITE(6,50)ADOT1
C
      ANGLE = ALPHA + THETA
      CALL U(ANGLE,RADIUS,CON,EI,UINF,AMU,ALPHA,U0)
      CALL DS(ANGLE,RADIUS,CON,AMU,X0,Y0)
      ANGLE = ANGLE - 0.0001
      CALL U(ANGLE,RADIUS,CON,EI,UINF,AMU,ALPHA,U1)
      CALL DS(ANGLE,RADIUS,CON,AMU,X1,Y1)
      ANGLE = ANGLE - 0.0001
      CALL U(ANGLE,RADIUS,CON,EI,UINF,AMU,ALPHA,U2)
      CALL DS(ANGLE,RADIUS,CON,AMU,X2,Y2)
      DS2 = SQRT((X2 - X1)**2 + (Y2 - Y1)**2)
      DS1 = SQRT((X1 - X0)**2 + (Y1 - Y0)**2)
      DS1 = DS1/CHORD
      DS2 = DS2/CHORD
C
C     FOR THE STAGNATION POINT COMPUTATION ONLY,
C     THE VELOCITY GRADIENT IS COMPUTED USING A
C     FORWARD DIFFERENCE PROCEDURE; THROUGHOUT
C     THE REST OF THE PROGRAM, THE VELOCITY
C     GRADIENT IS COMPUTED USING A CENTRAL
C     DIFFERENCE PROCE
C
      DUDS = (U1 - U0)/DS1
C
C     THE SECOND DERIVATIVE OF VELOCITY IS
C     COMPUTED USING A TAYLOR'S SERIES EXPANSION
C
      D2UDS2 = 2.* (U2 - U0)/((DS1 + DS2)**2) - (2./(DS1 + DS2))
     1    *((U1 - U0)/DS1)
C
C     ENTER INITIAL BOUNDARY LAYER PARAMETERS
C
      RLAMDA = 7.052
```

```
      ZZ = [illegible]
C
      DSS = DS1
      N = 5000
      ANGLE = ALPHA + THETA1 - [illegible]
      XOC = (X0 + XLE)/CHOR
      WRITE(6,1)XOC,U0,DUDS,D2UD32,F4,[illegible],ZZ,[illegible]
C
      ADOT = 0.0
      DO 10 J = 1,K
C
C     THE FUNCTION OF THIS LOOP IS TO COMPUTE THE
C     BOUNDARY LAYER PARAMETERS RIGHT AT THE STAG-
C     NATION POINT ON THE AIRFOIL.
C
C     THIS IS DONE TO ALLOW THE BOUNDARY LAYER TO
C     "STEADY OUT" BEFORE IT IS SUBJECTED TO A
C     PITCHING AIRFLOW. A VERY FINE COMPUTATION GRID
C     HAS BEEN SELECTED TO MINIMIZE THESE EFFECTS
C     ON THE COMPUTATIONS DOWNSTREAM OF THE STAG-
C     NATION POINT. ONCE THE BOUNDARY LAYER HAS
C     STEADIED OUT, COMPUTATION PASSES ON TO THE
C     PITCHING AIRFLOW.
C
C     NOT IMMEDIATELY SUBJECTING THE BOUNDARY LAYER
C     TO THE PITCHING AIRFLOW HAS NO APPRECIABLE
C     AFFECT ON [illegible] COMPUTATIONS, AS THE BOUNDARY
C     LAYER IS [illegible]ALLY VERY THIN (AS COMPARED TO
C     DOWNSTREA[illegible]ND THE GROWTH GRADIENT EVEN I[illegible]
C     THE UNSTEDY FLOW IS ABOUT THE SAME AS THE
C     GROWTH GRADIENT FOR STEADY FLOW, IN THE REGION
C     VERY NEAR THE STAG[illegible]TION POINT.
C
      N = N + 1
C
C     COMPUTE THE PERTINENT BOUNDARY LAYER PARAMETERS
C
      ZZ = DZDS*DSS+ ZZ
      RK = ZZ*DUDS
      FK = .47 - 6.* RK
      DZDS = FK/U1
C
      DELT = DSS/U1
      TIME = TIME + DELT
      DALPHA = DELT * ADOT
      ANGLE = ANGLE + DALPHA
      ALPH1 = ALPH1 + DALPHA
      CALL U(ANGLE,RADIUS,CON,EI,UINF,AMU,ALPHA,U2)
      DUDT = U2 - U1
      DUDT = DUDT/DELT
      ANGLE = ANGLE - 0.0001
      ANGLE1 = ANGLE - 0.0001
      CALL U(ANGLE1,RADIUS,CON,EI,UINF,AMU,ALPHA,U2)
      CALL DS(ANGLE1,RADIUS,CON,AMU,X2,Y2)
      ANGLE0 = ANGLE  + 0.0001
      CALL U(ANGLE0,RADIUS,CON,EI,UINF,AMU,ALPHA,U0)
      CALL DS(ANGLE0,RADIUS,CON,AMU,X0,Y0)
      CALL U(ANGLE,RADIUS,CON,EI,UINF,AMU,ALPHA,U1)
      CALL DS(ANGLE,RADIUS,CON,AMU,X1,Y1)
      DS1 = SQRT((X1 - X0)**2 + (Y1 - Y0)**2)
      DS2 = SQRT((X2 - X1)**2 + (Y2 - Y1)**2)
C
```

```
C
      DSS = (DS1 + DS2)/CHORD
      DUDS = (U2 - U1)/DSS
      UDUDS = U1 * DUDS
      XOC = (X2 + XLE)/CHORD
      IF(N.LT.5000) GO TO 10
      N = 0
      WRITE(6,1)XOC, U1, DUDS, DUDT, FK, RK, ZZ, ZZS
   10 CONTINUE
C
      ADOT = ADOT1
      N = 0
      DO 20 J = K1,K2
C
C     THIS LOOP COMPUTES THE BEHAVIOR OF THE BOUNDARY
C     LAYER AS IT IS SUBJECTED TO A PITCHING AIRFOIL.
C
C     THE TRANSIENT FLOW DYNAMICS ARE CARTURED BY
C     INCREMENTING THE FLOW ANGLE AT EACH POINT OF
C     COMPUTATION, I, BY AN AMOUNT
C
C          DALPHA = (PITCH RATE) * (TIME INCREMENT)
C
C     AT EACH POINT,THE BOUNDARY LAYER PARAMETERS
C     ARE COMPUTED, AS ARE THE ARC LENGTH, LOCAL
C     VELOCITY, TIME AND SPATIAL VELOCITY DE-
C     RIVATIVES, AND TIME INCREMENT. THE COMPUTATIONS
C     ARE CARRIED OUT FROM JUST PAST THE STAGNATION
C     POINT UP TO THE QUARTER CHORD POINT ON THE
C     SURFACE OF THE AIRFOIL, AT WHICH POINT THE
C     LOOP IS EXITED. COMPUTATION TO A DIFFERENT
C     POINT CAN BE ACHIEVED BY MERELY CHANGING
C     THE TEST CONDITION
C
      N = N + 1
C
C     COMPUTE THE PERTINENT BOUNDARY LATER PARAMETERS
C
      ZZ = DZDS*DSS+ ZZ
      RK = ZZ*(DUDS +DUDT/U1)
      FK = 0.47 - 6.*RK
      CALL POHL(RK,RLAMDA)
      DEL2 = 37./315. - RLAMDA/915. - (RLAMDA**2)/9072.
      F2K = (.3 - RLAMDA/10.)/DEL2
      DZDS = (FK + (4 + F2K) * ZZ * DUDT/U1)/U1
      DZDS = FK/U1
C
C     COMPUTE THE TIME INCREMENT FOR A PARTICLE
C     TO TRAVEL FROM POINT (I) TO POINT(I+1)
C
      DELT = DSS/U1
      TIME = TIME + DELT
      DALPHA = DELT* ADOT
       ANGLE = ANGLE + DALPHA
      ALPHI = ALPHI + DALPHA
      CALL U(ANGLE,RADIUS,CON,EI,UINF,AMU,ALPHA,U2)
C
C     COMPUTE THE UNSTEADY VELOCITY GRADIENT
C
      DUDT = (U2 - U1)/DELT
      ANGLE = ANGLE - 0.01
      ANGLE1 = ANGLE - 0.01
      CALL U(ANGLE1,RADIUS,CON,EI,UINF,AMU,ALPHA,U2)
      CALL DS(ANGLE1,RADIUS,CON,AMU,X2,Y2)
      ANGLE0 = ANGLE + 0.01
      CALL U(ANGLE0,RADIUS,CON,EI,UINF,AMU,ALPHA,U1)
      CALL DS(ANGLE0,RADIUS,CON,AMU,X2,Y2)
```

```
      CALL DS(ANGLE,RADIUS,C[illegible])
      CALL U(ANGLE,RADIUS,C[illegible])
      CALL DS(ANGLE,RADIUS,C[illegible])
C
C     COMPUTE ARC LENGTH AND VELOCITY GRADIENT
C
      DS1 = SQRT((X1 - X0)**2 + (Y1 - Y0)**2)
      DS2 = SQRT((X2 - X1)**2 + (Y2 - Y1)**2)
      DSS = (DS1 + DS2)/CHORD
      DUDS = (U2 - U0)/DSS
      DUDDS = U1 * DUDS
      XOC = X2 + XLE
      XOC = XOC/CHORD
C
C     STOP THE COMPUTATION AT THE QUARTER-CHORD
C
      IF(XOC.GE.0.250) GO TO 25
      IF(N.LT.250) GO TO 20
      N = 0
      WRITE(6,1)XOC, U1, DUDS, DUDT,     , RK, ZZ, DZDS
   20 CONTINUE
C
   25 WRITE(6,1)XOC, U1, DUDS, DUDT, RK, RK, ZZ, DZDS
      WRITE(6,45)ALPHI
      WRITE(6,55)PITCH
C     WRITE(6,60)RK
C     WRITE(6,70)DEL
C     WRITE(6,80)
C     WRITE(6,81)TIME
    1 FORMAT(4X,F6.3,2(4X,F10.3),4X,F7.3,4X,F7.4,4X,F8.4,2(4X,F4.3))
   30 FORMAT(1H1,"BOUNDARY-LAYER PARAMETERS FOR ",F6.2,"FT/SEC"/)
   40 FORMAT(" INITIAL ANGLE OF ATTACK: ",F5.3," DEGREES"/)
   45 FORMAT(/" FINAL ANGLE OF ATTACK: ",F5.3," DEGREES"/)
   50 FORMAT(" PITCH RATE: ",F7.3," DEGREES/SEC"/)
   55 FORMAT(" PITCH PARAMETER: ",F7.5/)
   60 FORMAT(" K AT THE QUARTER-CHORD: ",F8.4/)
   70 FORMAT(" R-L THICKNESS:  ",F9.3," FT"/)
   80 FORMAT(" TIME TO REACH THE QUARTER-")
   81 FORMAT(" CHORD FROM THE STAGNATION POINT: ",F7.5," SEC"/)
C
      STOP
       END
C
```

```
C
      SUBROUTINE U(ANGLE,RADIUS,CON,EI, [illegible]
      COMPLEX CMPLX,Z,EI,DZETA,[illegible]
C
C     THIS SUBROUTINE IS USED TO COMPUTE THE LOCAL
C     VALUE OF THE VELOCITY ON A JOUKOWSKI AIRFOIL.
C     USING COMPLEX POTENTIAL FLOW THEORY. IN THIS
C     THEORY, THE VELOCITY IS FIRST COMPUTED ABOUT
C     A CIRCLE IN THE COMPUTATION PLANE; THE GOV-
C     ERNING EQUATION IS THE DERIVATIVE OF THE
C     COMPLEX FLOW POTENTIAL EQUATION. ONCE THIS
C     VELOCITY HAS BEEN DETERMINED, THE VELOCITY
C     ABOUT THE CORRESPONDING AIRFOIL IS COMPUTED
C     BY:
C
C             U(AIRFOIL) = U(CIRCLE)/(DZ/DZETA)
C
C     WHERE DZ/DZETA IS THE DERIVATIVE OF THE
C     EQUATION USED TO TRANSFORM FROM THE CIRCLE
C     TO THE AIRFOIL.
C
C     THE COORDINATES AND VELOCITY IN THE CIRCLE
C     PLANE ARE COMPUTED:
C
      X = RADIUS * COS(ANGLE*CON)
      Y = RADIUS * SIN(ANGLE*CON)
      Z = CMPLX(X,Y)
      W = UINF *((1.,0.) - (RADIUS**2)/Z**2 +
     1  (2.* EI * RADIUS * SIN(ALPHA*CON))/Z)
      X = X + AMU
C
C     Z IS NOW CHANGED TO REPRESENT THE VALUES
C     OF THE COORDINATES USED IN THE TRANS-
C     FORMATION EQUATION:
C
      Z = CMPLX(X,Y)
      DZETA = (Z**2 - RADIUS**2)/Z**2
      UU = CABS(W)/CABS(DZETA)
      RETURN
      END
```

```
C
      SUBROUTINE DS(ANGLE,RADIUS,CON,AMU,X,Y)
      COMPLEX CMPLX,Z
C
C     THIS SUBROUTINE IS USED TO COMPUTE THE
C     ARC LENGTH BETWEEN TWO SPECIFIED POINTS
C     ON THE JOUKOWSKI AIRFOIL. USE IS MADE OF
C     COMPLEX VARIABLE THEORY TO DO THIS.
C
C     FIRST, POINTS OF INTEREST ARE COMPUTED ON
C     A CIRCLE, AND ARE THEN TRANSFORMED INTO
C     COORDINATES OF THE AIRFOIL BY THE EQUATION:
C
C             ZETA = Z + (RADIUS**2/
C
C     WHERE Z REPRESENTS THE COORDINATES (X,IY) OF
C     THE CIRCLE, AND ZETA REPRESENTS THE CO-
C     ORDINATES (XSI,IETA) OF THE AIRFOIL.
C
      X = RADIUS * COS(ANGLE+CON) + AMU
      Y = RADIUS * SIN(ANGLE+CON)
      Z = CMPLX(X,Y)
      Z = Z + (RADIUS**2)/Z
      X = REAL(Z)
      Y = AIMAG(Z)
      RETURN
      END
C
```

```
C
      SUBROUTINE POHL(RK,RLAMDA)
C     THE FUNCTION OF THIS SUBROUTINE IS TO COM-
C     PUTE THE VALUE OF THE SEPARATION PARAMETER,
C     LAMDA, GIVEN A VALUE OF K AS COMPUTED IN THE
C     MAIN PROGRAM. IN ACTUALITY, K IS A FUNCTION
C     OF LAMDA; HOWEVER, LAMDA IS NOT EXPLICITLY
C     COMPUTED IN THE POHLHAUSEN INTEGRATION THE--
C     AS K IS. THEREFORE, IT IS NECESSARY TO "PICK
C     OUT" VALUES OF LAMDA KNOWING K.
C
C     THIS SUBROUTINE BREAKS THE FUNCTIONAL RELATION-
C     SHIP BETWEEN LAMDA AND K INTO NEARLY UNIFORM
C     LINEAR OR 2ND ORDER FUNCTIONS AS APPROPRIATE.
C     THE VALUE OF K IS COMPUTED IN THE MAIN PRO-
C     GRAM AND IS THEN SENT TO THIS SUBROUTINE. THIS
C     VALUE OF K IS SUBJECTED TO SEVERAL PLACEMENT
C     TESTS TO DETERMINE THE APPROPRIATE REGION OF
C     THE LAMDA-VS-K CURVE. LAMDA IS THEN COMPUTED
C     THROUGH THE APPROPRIATE DESCRIBING RELATIONSHIP.
C
      RK1 = -.160
      RK2 = -.112
      RK3 = 0.00
      RK4 = 0.06
      RK5 = 0.076
      RK6 = 0.086
      RK7 = 0.0949
      IF(RK.LE.RK1) GO TO 10
      IF(RK.LE.RK2) GO TO 20
      IF(RK.LE.RK3) GO TO 30
      IF(RK.LE.RK4) GO TO 40
      IF(RK.LE.RK5) GO TO 50
      IF(RK.LE.RK6) GO TO 60
      IF(RK.GT.RK7) GO TO 70
C
      RLAMDA = .0149**2 - (RK - 0.08)**2
      RLAMDA = 12.- 100.*SQRT(RLAMDA)
      RETURN
C
   10 RLAMDA = (2./.012) * RK + 14.0
      RETURN
C
   20 RLAMDA = (4./.044) * RK + 2.18
      RETURN
C
   30 RLAMDA = (10./.14) * RK
      RETURN
C
   40 RLAMDA = 83.33 * RK
      RETURN
C
   50 RLAMDA = - 1.9 + 115. * RK
      RETURN
C
   60 RLAMDA = -6.54 + 176. * RK
      RETURN
C
   70 RLAMDA = 12.
      RETURN
      END
```

Vita

Richard G. Docken, Jr., was born on 7 August, 1956, at Wright-Patterson Air Force Base, Ohio, the son of Richard G. Docken and Shirley Mae Docken. He graduated from Fairmont West High School in 1974 and immediately enrolled at the Ohio State University in Columbus, Ohio. He received a Bachelor of Science Degree in Aeronautical and Astronautical Engineering and was commissioned into the Air Force Reserve in June 1978. He married the former Debra A. White the following August. He served his first tour of duty from August 1978 to May 1981 at the Air Force Weapons Laboratory, Kirtland Air Force Base, New Mexico, first as a Laser Systems Project Officer and then as a System Acquisition Management Officer.

Permanent Address: 7645 Stancrest Drive
Huber Heights, Ohio 45424

This thesis was typed by Mrs. Debra Docken.

SECURITY CLASSIFICATION OF THIS PAGE (When Data Entered)

REPORT DOCUMENTATION PAGE

READ INSTRUCTIONS BEFORE COMPLETING FORM

1. REPORT NUMBER
AFIT/GAE/AA/82D-9

2. GOVT ACCESSION NO.
AD-A124716

3. RECIPIENT'S CATALOG NUMBER

4. TITLE (and Subtitle)
GUST RESPONSE PREDICTION OF AN AIRFOIL USING A MODIFIED VON KARMAN-POHLHAUSEN TECHNIQUE

5. TYPE OF REPORT & PERIOD COVERED
MS Thesis

6. PERFORMING ORG. REPORT NUMBER

7. AUTHOR(s)
Richard G. Docken, Jr.
Caption, USAF

8. CONTRACT OR GRANT NUMBER(s)

9. PERFORMING ORGANIZATION NAME AND ADDRESS
Air Force Institute of Technology (AFIT-EN)
Wright-Patterson AFB, Ohio 45433

10. PROGRAM ELEMENT, PROJECT, TASK AREA & WORK UNIT NUMBERS

11. CONTROLLING OFFICE NAME AND ADDRESS

12. REPORT DATE
December 1982

13. NUMBER OF PAGES

14. MONITORING AGENCY NAME & ADDRESS(if different from Controlling Office)

15. SECURITY CLASS. (of this report)
Unclassified

15a. DECLASSIFICATION/DOWNGRADING SCHEDULE

16. DISTRIBUTION STATEMENT (of this Report)

Approved for public release - distribution unlimited

17. DISTRIBUTION STATEMENT (of the abstract entered in Block 20, if different from Report)

18. SUPPLEMENTARY NOTES
Approved for public release: IAW AFR 190-1
LYNN E. WOLAVER
Dean for Research and Professional Development
Air Force Institute of Technology
Wright-Patterson AFB, Ohio
6 JAN 1983

19. KEY WORDS (Continue on reverse side if necessary and identify by block number)

Gust Response
Rotating Airflow
Rotating Airfoil
Momentum-Integral Equation for Unsteady Flow
von Karman-Pohlhausen Technique
Unsteady Flow
Boundary Layers

20. ABSTRACT (Continue on reverse side if necessary and identify by block number)

An analytical study is presented regarding the theoretical behavior of an airfoil in a pitching airflow. The theoretical development includes the momentum-integral equation for boundary layers in unsteady flow and the von Karman-Pohlhausen integral method for unsteady flow. A computer program was written to model this and was applied to a symmetric Joukowski airfoil. The results of this study show a linear relationship between the increase in the stall angle of attack and the non-dimensional pitch rate, $\frac{1}{2}C\dot{\alpha}/U$.

DD FORM 1 JAN 73 1473 EDITION OF 1 NOV 65 IS OBSOLETE

SECURITY CLASSIFICATION OF THIS PAGE (When Data Entered)

7. For this study, repeat steps 3 through 6 until:

END

FILMED

3-83

DTIC